REPORT OF ON-BOARD MEASUREMENT CAMPAIGNS

Kati Lehtoranta

Niina Kuittinen

GREEN RAY

Funded by the European Union

Funded by the European Union. Views and opinions expressed are however those of the author(s) only and do not necessarily reflect those of the European Union or CINEA. Neither the European Union nor CINEA can be held responsible for them.

DELIVERABLE DESCRIPTION

Grant Agreement Number	101056642
Project Acronym	GREEN RAY
Project Title	New GeneRation marinE ENgines and Retrofit solutions to Achieve methane abatement flexibilitY
Project Call	HORIZON-CL5-2021-D5-01-12
Project Duration	60 months: 1 June 2022 – 31 May 2027
Deliverable Number	D1.2
Deliverable Title	Report of on-board measurement campaigns
Deliverable Type	Report
Security Classification	Public
Contributing Work Package	WP1
Lead Partner	VTT
Contributing Partners	MSC, CdA, WFI, FMI
Version	v1
Authors	Kati Lehtoranta, Niina Kuittinen
Reviewers	
Contractual Delivery Date	31 May 2024

GREEN RAY

Keywords list:
Methane slip, shipping, emission measurements, on-board, liquified natural gas

GREEN RAY Consortium

VTT (Teknologian Tutkimuskeskus VTT Oy)

FMI (Ilmatieteen Laitos)

Shell (Shell Global Solutions International BV)

CdA (Chantiers De L'Atlantique)

WIT (Wärtsilä Italia Spa)

WFI (Wärtsilä Finland Oy)

DNV (DNV AS)

MSCMYM (MSC Malta Yard Management Ltd)

CMA (CMA Ships)

WSCH (Wärtsilä Services Switzerland AG)

MSC (MSC Cruise Management UK Limited)

REV (Revolve Water)

Table of Contents

1. Introduction

Liquified natural gas (LNG) is considered as one fuel pathway in decarbonization of the maritime industry and meeting emission targets. LNG is mainly composed of methane, which is a lightweight, energy-dense hydrocarbon with high hydrogen to carbon ratio. Currently, LNG is produced from fossil origins, however, methane as a molecule can also be produced from biobased origins or be formed synthetically.

Several types of marine engines have the capability to use LNG as fuel. The most common technology utilized in ships main engines is the low-pressure dual-fuel technology (LPDF) (Kuittinen et al., 2023a) which can be utilized in both 4-stroke (4-S) and 2-stroke engines (2-S) and allows utilization of both gaseous and liquid fuels. In previous studies, LNG use in LPDF 4-S marine engines has been shown to decrease both climate relevant emissions of carbon dioxide (CO_2, by 18%) and black carbon (BC, by 97%) as well as local air pollutants such as nitrogen oxides (NO_x, by 93%) and particulate matter (PM, by 97%) compared to the use of liquid fuels (Peng et al., 2020). LNG use has also been shown to be able to reduce the specific emission of non-volatile particle number above 23nm ($PN_{nv,<23nm,}$ by 98-99%) and total particle number (by 40-59%) compared to liquid distillate fuels (Kuittinen et al., 2021; Lehtoranta et al., 2019). However, the emission of unburned methane originating from the LNG has been recognized as an issue which can partly undermine the benefits of LNG use in these engines (Grönholm et al., 2021; Peng et al., 2020; Stenersen & Thonstad, 2017; Ushakov et al., 2019). Methane is a strong greenhouse gas (GHG) with global warming potential (GWP) of 29.8 times that of CO_2 on the 100-year timescale (IPCC, 2022). Overall, the amount of methane slip information from new engines is limited (Kuittinen et al., 2023a).

In the European Union, maritime transport accounts for 75% of the external trade by volume and 400 million passengers embark or disembark in the EU ports, including 14 million cruise passengers. While maritime transport has been reported to remain the most carbon-efficient mode of transport, the ship traffic to or from ports in the European Economic Area accounts for 11 % of all European Union carbon dioxide emissions from transport and 3-4 % of total CO_2 emissions. (FuelEU Maritime, 2023). In order to mitigate the methane emitted from marine engines, the European Union has recently introduced two regulations where methane is included. Firstly, the FuelEU Maritime requires ship owners to report their methane emissions together with fuel consumption. In the regulation, a predefined methane slip value as percentage of consumed fuel is assigned for each LNG engine technology. Alternatively, the ship owners have a possibility to utilize methane slip value verified by direct measurement from their ships. Secondly, maritime transport will be part of the EU Emissions Trading Scheme (ETS) from the beginning of 2024. In the beginning, ETS will consider emitted CO_2 but in 2026, methane will be added to the list of GHGs considered (European Commission, 2024). Globally, methane is considered by the International Maritime Organization (IMO) in the draft guidelines on life cycle GHG intensity of marine fuels (IMO 2023).

In this report, methane slip is investigated on-board two newbuild LNG vessels applying new standard engines and an engine with new combustion concept. In addition to methane slip, the total greenhouse gases were studied, together with other airborne gaseous and particulate emissions. The information gained through steady load measurements, normal engine operation as well as by following the 8-month activity profile of the engine may be utilized in decision making as well as improving the emission inventories and modelling of methane slip from the current vessel fleet. Furthermore, the results are immediately useful to project partners developing new technologies to reduce methane slip.

2. Target

On board measurements are planned for the cases where there is a lack of information. Three important aspects were planned to include into the measurement campaign onboard:

- Firstly, to have new data and emissions results of a new, state-of-the-art, marine engine.
- Secondly, to have real emissions measured onboard during vessel normal operation.
- Thirdly, to have data and emission results of different engine loading, including dynamic loads occurring during vessel normal operation (e.g. in maneuvering and berthing).

Measurement of methane emissions is the primary focus in the onboard measurements. To answer the goals of the call more widely the emission studies will cover not only methane, but also other GHG emissions like CO_2, N_2O. To have a comprehensive overall picture of all the emissions that are formed from LNG combustion, the pollutants, NOx and particle emissions, including black carbon (BC) are measured onboard as well.

Black Carbon has both, effects on climate as well as on air quality. The importance of BC emissions from shipping has been acknowledged by IMO as well and limit values are anticipated. BC emissions from LNG engines are extremely low based on limited number of measurements. Particularly for new LNG vessels, reliable BC emission data is needed for evaluation of climate impact of new LNG fleet.

The measurement methods applied for onboard studies in the GREEN RAY project will follow the ISO 8178 / NOx technical code for CO_2 and NOx measurements, meaning CO_2 is measured by non-dispersive infrared and NOx by chemiluminescence. Black carbon is measured with methods included in candidate methods selected by the IMO in the 5th PPR meeting, 2018. The methane (slip) itself will be measured by gas chromatography while a Fourier transformation infrared (FTIR) spectrometer is to utilize for methane measurement also. Formaldehyde is to be measured by FTIR as well.

Natural gas combustion is known to possibly produce aldehyde emissions but only few have measured that onboard an LNG vessel. Adding this aldehyde measurement to the current scope will provide new knowledge of the levels formed during normal vessel operation, which is important to consider, due to the health effects especially in coastal areas. Moreover, this information about the aldehyde formation can be utilized by technology developers to avoid aldehyde formation together with diminishing methane.

Particle emissions are measured following ISO 8178 for particle mass measurements, this is also the measurement method required by European emission standards for engines in inland waterway vessels. The Stage V emission standards for engines in inland waterway vessels introduced a limit for particle number and in current study we add this particle number measurements for the onboard studies as well. Besides currently regulated PN size class of >23nm, measurements cover anticipated regulation of >10nm size class.

This task will contribute to understanding what the methane slip and other emissions from newer vessels (current state of art) is. The results of the experiments are immediately provided to WPs 2-4 to make use of them in technology development preventing methane slip.

3. Experiments

3.1. Measurement methods

3.1.1. Instruments on-board

During on-board campaigns, several measurement instruments were installed on-board to study methane together with other emission compounds. List of the applied instruments is given below.

- Micro Gas Chromatograph

Methane, ethane, ethene, and propane concentrations were quantified by gas chromatograph (Agilent 490 Micro Gas Chromatograph) where small amount of sample is injected every 2 min and concentrations detected downstream a separation column. The detection limits of the instrument are 10 ppm for methane and 2 ppm for ethane, ethene, and propane.

- Fourier Transform Infrared Spectrometer

More than 10 gaseous compounds were measured on-line at 20 seconds intervals using Fourier transformation infrared (FTIR) equipment (Gasmet DX-4000). The FTIR was applied to study methane together with formaldehyde, NO, NO_2, N_2O, CO, and water. The compounds measured with FTIR include also sulphur dioxide (SO_2). Two FTIR units were applied in both campaigns for comparison and for studying the effect of selective catalytic reduction unit in the second campaign. The instrument can detect concentrations above 2 ppm for methane, 2 ppm for formaldehyde, 10 ppm for NO, 3 ppm for NO_2, 4 ppm for N_2O, 3 ppm for CO, 3 ppm for SO_2 and 0.06% for H_2O.

- Horiba PG-250A analyzer

The HORIBA PG-250 gas analyzer was applied for measuring NO_x, SO_2, CO, CO_2, and O_2. These include NDIR (pneumatic) for CO and SO_2; NDIR (pyrosensor) for CO_2; chemiluminescence (cross flow modulation) for NO_x; and paramagnetic cell for O_2 measurements.

- Ecophysics CLD

Nitrogen oxides were measured by a standard method applying chemiluminescence detector (CLD, ECO PHYSICS CLD 8xx). Detection limit of the device is 0.25 ppm when 0-5000 ppm range is applied.

- Engine Exhaust Diluter and Condensation Particle Counters

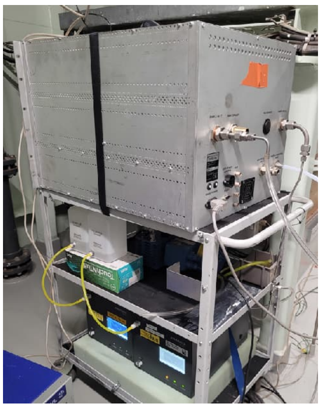

To study particle number (PN), the sample was conditioned and diluted with the Dekati Engine Exhaust Diluter (DEED). In dilution unit the sample is diluted in two stages to decrease the particle concentration low enough for the particle counter. Device meets the current legislative demands for vehicle type approval measurements. In the DEED, the first of the two ejectors in the system was heated to 200°C. The particle number concentration was then measured with the Airmodus A23 condensation particle counter (CPC), with a cut-point of 23 nm, considered also in the EU Stage V regulation. In addition, Airmodus A20 with 10 nm cut-point was utilised in parallel with the other CPC. The measurement range of the CPCs is 0 – 100 000 1/cm^3.

- Micro Soot Sensor

Black carbon (BC) was measured utilizing thermal optical measurement principle (AVL Micro Soot Sensor, MSS). The Micro Soot Sensor is a system for continuous measurement of soot concentrations in the exhaust gas from internal combustion engines. The MSS utilizes photoacoustic measurement method. The measurement range of the instrument is from 1 µg/m^3 to 50 mg/m^3.

- eDiluter

Dekati eDiluter is a portable dilution system which is based on two stage dilution where the first dilution stage is heated. Each dilution stage consists of an ejector diluter with additional sheath air flow. The use of a large ejector nozzle and sheath air minimizes particle losses within the system. The first dilution stage of Dekati eDiluter could be utilized to dilute the sample prior to DEED and MSS. The dilution air was heated to 250°C.

- VTT SDS Ship dilution and sampling system

Particle mass (PM) was studied by collecting exhaust aerosol to filters (Pallflex TX40HI20-WW filters with o.d. 47 mm). A portable ship dilution system (SDS) was used to condition the sample following the ISO 8178 protocol. The SDS is a partial flow dilution system intended for gravimetric sampling of exhaust particulates from internal combustion engines. For each load point, 3-4 filter samples were collected.

3.1.2. Calculation of emission factors

To convert the measured concentrations into brake specific emission factors, the engine power, together with fuel consumption data of both main and the pilot fuel was utilized. In the case when two engines were located in the same engine room with a common fuel flow meter, the other engine remained inactive during the measurements, allowing direct metering of the fuel flow. The composition of the LNG was retrieved from bunkering report. For the pilot fuel (and MGO), a sample of the pilot fuel was collected on-board and analyzed in laboratory for its C, H, and N content. The fuel consumption together with composition were then used to calculate the exhaust gas mass flow rate by the carbon balance method (e.g. ISO 8178 and NO_x technical code).

Total greenhouse gas emissions were calculated for steady load conditions, including carbon dioxide together with methane and black carbon. To convert methane and black carbon to CO_2 equivalents, the 100-year CO_2 equivalent global warming potential value of 29.8 was applied for methane (IPCC, 2022) and 900 (Bond et al., 2013) for BC.

3.2. On board campaign #1 / RoPax Ferry Aurora Botnia

The onboard campaign was conducted on board Aurora Botnia, Wasaline's RoPax ferry operating the route between Vaasa (Finland) and Umeå (Sweden), in December 2022 with a planning schedule presented in Table 1 below. This modern, state-of-the-art ferry was built in 2021, starting its operation in autumn 2021. The ferry is operated by four Wärtsilä 31DF dual-fuel engines capable of operating on LNG. These engines are medium-speed 4-stroke marine engines and have 8 cylinders with a power of 550 kW per cylinder. One of the engines was piloting a new combustion concept while the others were standard setups built on 2021. According to the engine manufacturer, the engine piloting new combustion concept involves precise controlling of the engine in aiming to achieve reductions in exhaust emission levels.

Both engines, standard and new combustion concept engine, were included in the onboard studies. The first measurement day was scheduled to study the emissions during vessel normal operation on its normal operation route between Vaasa and Umeå (Error! Reference source not found. 1). Two days were planned to study the emissions from different engine loadings from both engines. The target with different engine loadings was to study: the lowest practical/possible load mode, 25%, 50%, 75% and the highest possible load mode.

Table 1. Schedule of measurements on-board Aurora Botnia

Date	Trip schedule			Engine
3.12.	Vaasa-Umeå	16:30-19:00	VTT boarding 16:00, unpacking	
	Umeå-Vaasa	20:15-01:00		
4.12.	Vaasa-Umeå	08:00-11:00	Installations	
	Umeå-Vaasa	13:00-18:00	Installations + testing	
	Vaasa-Umeå	20:00-23:00		
5.12.	Umeå-Vaasa	11:00-16:00	'normal operation'	new engine
	In Vaasa	16:00-20:00	'normal operation'	new engine
	Vaasa-Umeå	20:00-23:00	'normal operation'	new engine
6.12.	Umeå-Vaasa	08:00-12:30	different engine loadings	new engine
	Vaasa-Umeå	13:15-15:45	different engine loadings	new engine
	Umeå-Vaasa	16:45-21:15	back up time	new engine
	Vaasa-Umeå	22:15-00:45		
7.12.	Umeå-Vaasa	08:00-13:00	different engine loadings	standard engine
	Vaasa-Umeå	14:30-17:30	different engine loadings	standard engine
	Umeå-Vaasa	19:00-00:00	normal operation	standard engine
8.12.	Vaasa-Umeå	08:00-10:30	back up time	standard engine
	Umeå-Vaasa	11:15-16:00	uninstallations	

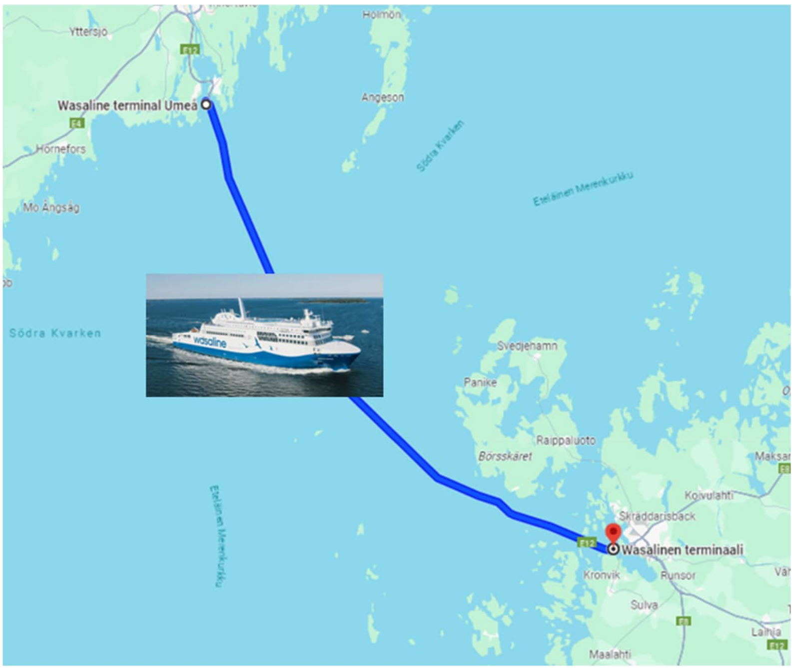

Figure 1. The Aurora Botnia route between Vaasa, Finland and Umeå, Sweden. Map from Google Maps.

LNG was utilized as the primary fuel and marine diesel oil (MDO) as the pilot fuel (Table 2, Table 3 The methane content of the LNG was high i.e., 95.1%. The MDO had a very low sulfur level containing only 0.01% of sulfur.

MDO usage as a pilot fuel contributed to around 3-28% of the total fuel flow depending on the engine and engine loading. With ME4 the share of pilot fuel was 3-13% and with ME3 piloting the new combustion concept, the share of pilot fuel was 10-28%. With both engines the higher proportions of MDO were at the lowest loads.

Table 2. Main specifications of LNG used on board.

methane (mol-%)	95.1
ethane (mol-%)	4.1
propane (mol-%)	0.6
nitrogen (mol-%)	0.1
ibutane (mol-%)	0.07
nbutane (mol-%)	0.07
carbon dioxide (mol-%)	0.00
density (kg/m^3)	0.75

Table 3. Main specifications of MDO used on board.

carbon (m-%)	84.4
hydrogen (m-%)	14.0
nitrogen (m-%)	0.06
sulphur (m-%)	0.01
density at 15 °C (kg/m^3)	877.4
viscosity at 80 °C (mm^2/s)	2.87

Raw exhaust gas was sampled from one measurement point in the exhaust pipe with few meters distance from the engine and was then divided to separate devices, equipped with different sampling conditioning, measuring both gaseous and particle emissions (Figure 2, see chapter 3.1 for measurement devices).

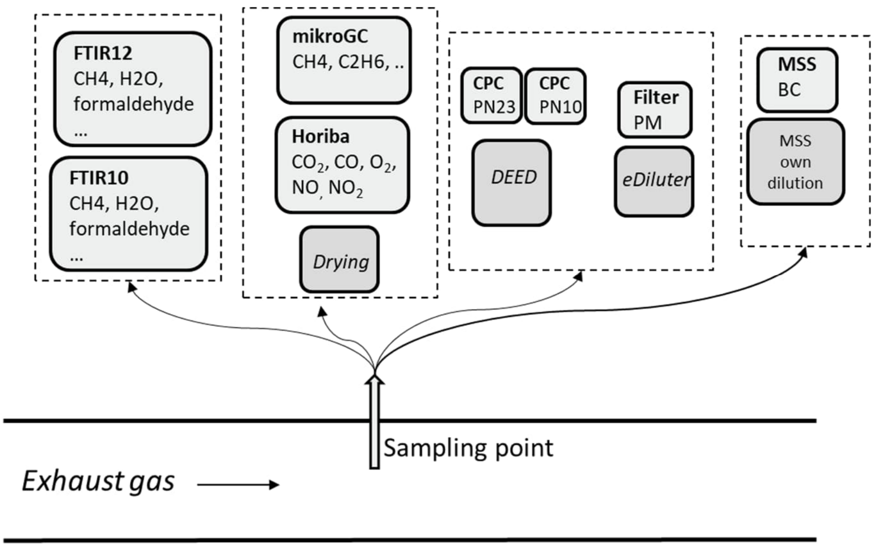

Figure 2. Schematic of the instrument installations on-board.

3.3. On board campaign #2 / Cruise Ship World Europa

The second campaign took place on-board the cruise ship MSC World Europa, a state-of-the-art cruise ship fueled by LNG, during its one-week itinerary on the Mediterranean. MSC World Europa is a newbuild cruise ship who begun its service in December 2022. The planning of the measurements started in early 2023 and the actual measurement campaign was conducted in May 2023. Planning of the measurements was conducted primarily by VTT in close co-operation with MSC and CdA to define the suitable vessel, engine, measurement period, suitable locations for the instruments on-board, transfer of data and fuel samples between MSC and VTT, and plan for operating in collaboration with the Genoa harbor for on boarding the vessel. Extended measurement plan was created by VTT to define e.g., the instruments and gases to be brought on-board, schedule and targeted load conditions as well as sampling points in the exhaust line. The route of the vessel during the measurement campaign is shown in Figure 3.

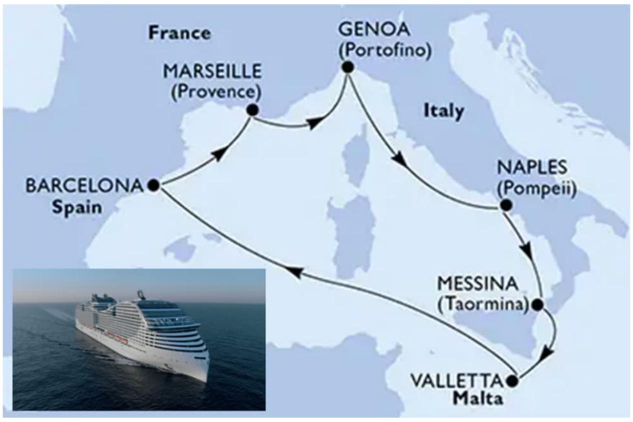

Figure 3. Route of MSC World Europa during the on-board measurements.

The MSC World Europa is equipped with five main engines which are Wärtsilä 46DF, 14-cylinder, 600 rpm, 4-stroke low pressure dual-fuel engines with output of 16 030 kW. The LPDF engines apply a pilot injection of liquid fuel to ignite the mixture of air and natural gas. The diesel generator 5 (DG5) out of the five engines on-board was chosen for the measurements. In this campaign it was possible to compare the operation of the dual-fuel engine both during operation on LNG and in diesel mode, utilizing marine gas oil (MGO) for combustion. On the MSC World Europa, engines are divided into two separate engine rooms having either 2 or 3 engines, and fuel consumption is measured by the engine room. To have direct measurement of the fuel usage of the engine to be studied in the campaign, only one engine in the engine room could be used at a time. For this reason, the engine room with two engines was chosen, and the other diesel generator remained inactive during the campaign, allowing direct reading of the fuel meter. During the campaign, the engine was mainly fueled by LNG with the pilot injection of MGO but could also switch to MGO to allow emission characterization during full MGO operation. The composition of the LNG used during the campaign was retrieved from bunkering report and it contained 97.6 mol-% methane, 1.9 mol-% ethane, and 0.2407 mol-% propane. The MGO used as pilot fuel had low sulfur content of 0.03%. The properties of the fuels used during the campaigns are shown in Table 4 and Table 5.

Table 4. Composition and properties of the LNG used during the campaign.

Compound	Share		
Methane	CH_4	97.5773	mol-%
Ethane	C_2H_6	1.9067	mol-%
Propane	C_3H_8	0.2407	mol-%
n-Butane	n-C4	0.0821	mol-%

i-Butane	n-C4	0.0845	mol-%
n-Pentane	n-C5	0.0071	mol-%
t-Pentane	n-C5	0	mol-%
neo-pentane	n-C5	0	mol-%
n-Hexane	C6+	0	mol-%
Nitrogen	N2	0.1016	mol-%
Carbon dioxide	CO2	na	mol-%
Sulfur	H2S	na	mg/nm3
Oxygen	O2	na	mol-%
Fuel properties			
Density (RKM@-158.7C)		427.049	kg/m3
HHV Gross calorific value		40.664	MJ/nm3
LHV Net calorific value		36.674	MJ/nm3
Gross Wobbe-index		54.353	MJ/nm3
Net Wobbe-index		48.597	MJ/nm3
HHV Gross calorific value		55.221	MJ/kg
LHV Net calorific value		49.802	MJ/kg

Table 5. Properties and composition of the MGO used during the campaign.

Fuel properties		
Density at 15C	836.9	kg/m3
Sulfur	0.03	%m/m
Viscosity, 40C	2.568	mm2/s
Flash Point	66	°C
Pour point	-18	°C
Carbon	86.7	%m/m
Hydrogen	13.5	%m/m
Nitrogen	0.004	%m/m

During the campaign, emission measurements were conducted both during steady engine load conditions and during normal engine operation when the vessel was operating at open sea or arriving, residing, and departing harbors. Five steady load conditions were measured with both fuels, being 12, 25, 54, 75, and 80% for LNG operation and 10, 25, 54, 75, and 80% from MGO operation with ±2 %-unit accuracy. In the case of LNG operation, the load conditions of 54% and 80% were repeated on two separate days. The continuous data of engine power and consumption of both main and pilot fuel were received from the ship owner MSC in 5 min time resolution and was applied in calculating specific emissions during steady load conditions. For studying the emissions under normal engine operation, the same load and fuel consumption data in 1s time resolution could be received from the ship manufacturer CdA. During these normal operation periods, no requests were made to vessel personnel regarding engine use, but they operated the engine according to the momentary power needs of the vessel to maintain the cruise schedule and the operations on-board. During the normal operation measurements, the vessel spent majority of the time cruising at open sea, but also departed from and arrived at several harbors as well as resided in harbors. During the normal operation, the vessel operated on LNG but on few occasions the engine momentarily switched to liquid fuel mode and combusted MGO. The schedule including the measurement days and realized test conditions including used fuel, engine, and engine load is shown in Table 6.

Table 6. Schedule and descriptions of measurements conducted on-board MSC World Europa.

DATE	Test description	Fuel	Engine	Engine load %
15.5.2023	Normal operation	LNG	DG5	
16.5.2023	Normal operation	LNG	DG5	
16.5.2023	25% load MGO	MGO	DG5	25
16.5.2023	Normal operation	LNG	DG5	53
17.5.2023	10% load LNG	LNG	DG5	10
17.5.2023	25% load LNG	LNG	DG5	25
17.5.2023	54% load LNG	LNG	DG5	54
17.5.2023	Normal operation	LNG	DG5	
17.5.2023	82% load LNG	LNG	DG5	82
17.5.2023	Normal operation	LNG	DG5	
18.5.2023	82% load MGO	MGO	DG5	
18.5.2025	Normal operation	LNG	DG5	82
19.5.2023	25% load MGO	MGO	DG5	25
19.5.2023	10% load MGO	MGO	DG5	10
19.5.2023	50% load MGO	MGO	DG5	50
19.5.2023	Normal operation	MGO->LNG	DG5	
19.5.2023	75% load LNG	LNG	DG5	75
19.5.2023	75% load MGO	MGO	DG5	75
19.5.2023	Normal operation	MGO->LNG	DG5	75
20.5.2023	Normal operation	LNG	DG5	

The focus in the second onboard campaign was to study the methane levels in these different operation conditions, while other gaseous and particle emissions were measured as well. The measurements were conducted by sampling engine exhaust through a sonde installed to a connector port on the deck above the engine room. The exhaust was then split to instruments measuring both gaseous and particulate emissions. Schematic of the instrument installations is shown in Figure 4. For comparison, and to study the exhaust concentrations downstream selective catalytic reduction (SCR), one FTIR instrument of was installed on an upper deck of the vessel. A sonde connected to heated sampling line for the second FTIR was installed above the SCR outlet.

Prior to the campaign, the same system was built in VTT laboratory to test the equipment and apply suitable analysis methods for the analyzers as well as test the calibration gas cylinders to be brought on-board.

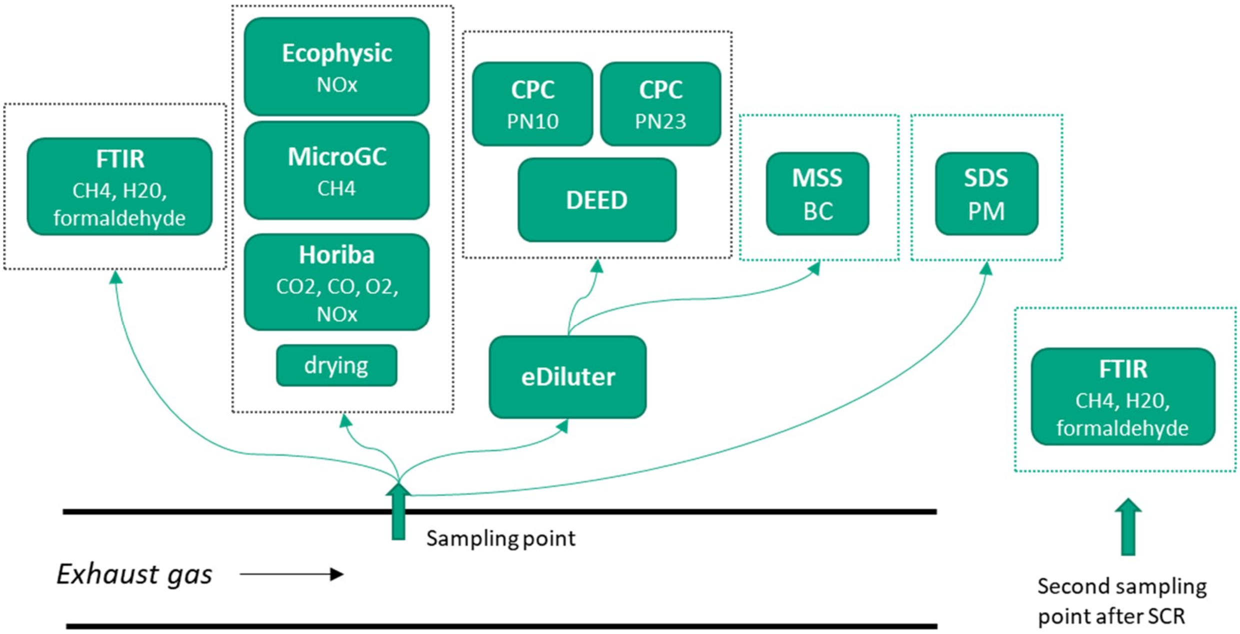

Figure 4. Schematic of the instrument installations on-board. Majority of instruments was installed few meters downstream the engine and one FTIR instrument to a second sampling point downstream the SCR.

In the second campaign, more focus was given to measuring the normal operation of the engine. In addition, an 'Actual operation' cycle was developed, based on 8 months of engine data received from the vessel manufacturer CdA. For this, the engine loads were extracted from the vessel Data Acquisition System (DAS) in 1Hz time resolution for the 8-month period between April 12th and December 15th 2023 when the vessel was all the time operating in the Mediterranean. One-minute averaged data was used to calculate the profile of engine operation time on different load conditions. The relative time spent at different engine loads was then used for weighing the emission, similarly to previous studies (Peng et al., 2020; Rochussen et al., 2023). For comparison, specific emissions of methane and total GHGs including carbon dioxide, methane, and black carbon was also calculated applying weighting factors defined in the E2 and D2 test cycles for which the studied engine is certified. However, the engine loads were adjusted, utilizing the studied engine load conditions instead of the load conditions defined in the cycles ((10), 25, 50, 75, and 100%). During low engine load conditions of 20-35%, the engine utilization was observed to be transient as the load condition was being continuously adjusted during arrivals and departures from harbors. Therefore, an emission factor for this 'Normal 20-35% loads' operation was calculated based on measurements of 4 departures, 4 arrivals and 1 stop at sea. The normal operation emission factor was then utilized in the calculation of the actual weighted emission, whereas emissions at steady 25% load was utilized for the adjusted E2 and D2 cycles.

4. Results

4.1. On board campaign #1 / RoPax Ferry Aurora Botnia

4.1.1. Methane and other gaseous emissions under steady load conditions

Measurement of methane was conducted with two parallel instruments GC and FTIR. In Figure 5 we present the calculated methane emissions (g/kWh) measured with both instruments for both engines as a function of engine load. First, this shows that similar methane levels were measured with both instruments increasing confidence in these results. Second, this shows lower methane levels at higher engine loads compared to especially the lowest engine load of 10%, with both engines. And third, this shows lower methane levels recorded from the engine with the new combustion concept. At the engine loads of 50-90% the new combustion engine produced 50-65% less methane compared to the standard engine and at the lower loads (with higher absolute methane levels) the difference between the engines was even higher. At 10% load, the engine with the new combustion concept produced methane emission below 4 g/kWh while at the same load condition with the standard engine the methane emission was over 12 g/kWh.

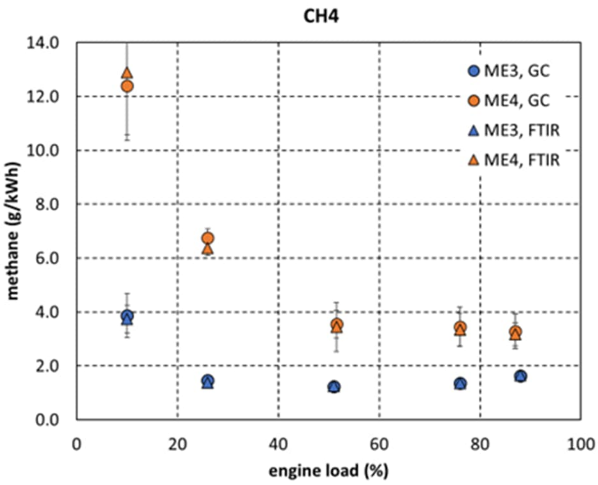

Figure 5. Methane emissions measured with GC (dots) and FTIR (triangles) – for both engines, ME3 and ME4, as function of engine load. Error bars show the standard deviations.

In addition to methane, other hydrocarbons (ethane, propane and ethene) were also analyzed with the GC. As expected much lower emission values were seen for all other hydrocarbons compared to the methane emission. With the ME4, ethane, propane and ethene were found in the exhaust gas, while with the ME3 only ethane was found. With ME3, the concentrations of other hydrocarbons than methane and ethane, were such low that they are below the detection limit of the GC in use. Detection limit for ethane and propane being approx. 2 ppm. Calculating the portions of different hydro-carbon components from the total hydrocarbon emissions of the ME4 exhaust results to 95.1-95.9 mol-% of methane, 3.2-3.8 mol-% of ethane and 0.44-0.56 mol-% of propane. Comparing these to portions found in the LNG fuel (Table 1: methane 95.1 mol-%, ethane 4.1 mol-% and propane 0.6 mol-%) shows that these are on the same level.

NOx, CO, and CO_2 emissions, for both engines, as a function of engine load, are presented in Figure 6. From the FTIR data, also the formaldehyde was analyzed, and this is included in Figure 6. This shows that NOx emissions are significantly smaller from ME3 compared to ME4, since NOx levels were below 0.5 g/kWh with ME3 at all loading conditions, while with ME 4, NOx was 2-4 g/kWh at 25-90% load and higher (close to 18 g/kWh) at lowest load of 10%. CO_2 emission was found to be slightly higher with the ME3 compared to ME4. CO and HCHO emissions behaved similarly to the methane emissions, showing highest levels at lowest loads and with ME3 both CO and HCHO were found to be on a lower level than with ME4, at all studied engine loads.

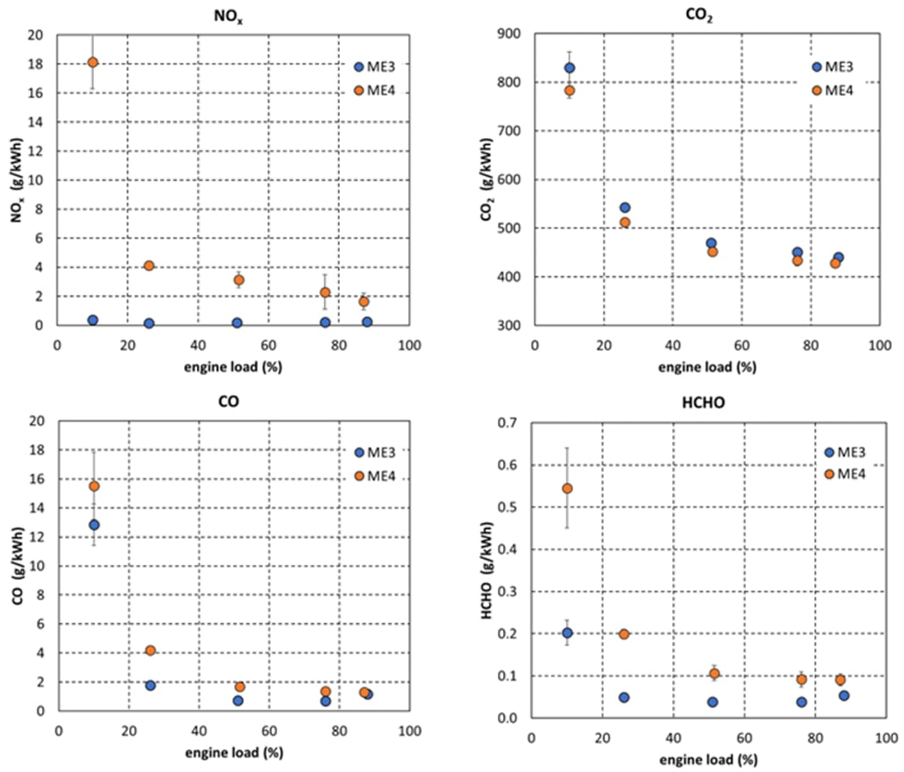

Figure 6. NOx, CO_2, CO, and formaldehyde (HCHO) emissions for both engines ME3 and ME4 as a function of engine load. Error bars show the standard deviations.

With FTIR, also N_2O was measured. However, in all measurement points of present study, the FTIR showed values below 2 ppm for N_2O which are all below the reliable detection limit of the FTIR device is use.

4.1.2. Particle emissions under steady load conditions

In addition to gaseous emission measurements particle emissions were studied with continuous PN measurement. Both the $PN_{>23nm}$ and $PN_{>10nm}$ concentrations were studied and are presented in Figure 7 as 1/kWh as a function of engine load for both engines studied. The lowest particle emission levels were recorded at the higher loads of 75% and 90%, while the emission levels increase at the lower loads. ME3 with the new combustion concept is showing higher particle emission levels than the ME4 (standard engine setup).

As anticipated, the $PN_{>10nm}$ is showing higher concentrations compared to $PN_{>23nm}$, covering the particles in the size range of 10-23 nm in addition to $PN_{>23nm}$. Especially at the lower loads of 10-50%, the difference between the $PN_{>10nm}$ concentrations of ME3 and ME4 is less than what is observed in the case of $PN_{>23nm}$ concentrations. Thus, considering the fraction of 10-23 nm particles in addition to 23 nm increases the total particle number by 142-680% in the case of ME4, whereas in the case of ME3 the addition is 70-306%.

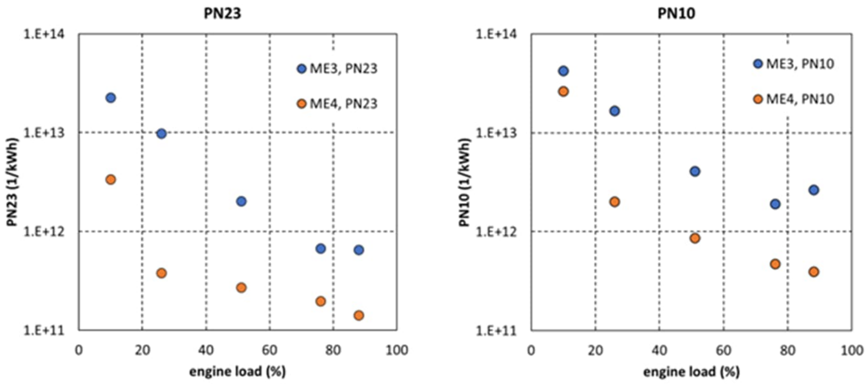

Figure 7. Particle number emissions as function of engine load for both engines ME3 and ME4. PN23 de-notes particles larger than 23nm and PN10 particles larger than 10nm in diameter.

Note. The PM measurement was not possible to conduct reliably onboard Aurora Botnia, due to short time available, as sampling one PM takes already 30-45min and for reliable measurement, at least 3 repetitions would have needed. Also, unluckily, due to a human error, the black carbon measurement data was not saved during all the days onboard Aurora Botnia. This is why we do not present any PM or BC results here.

4.1.3. Total greenhouse gas emissions

To have a better overview of the total GHG emissions, we combined the CO_2 and CH_4 results, calculating the CH_4 as CO_2 equivalent utilizing the 100-year global warming potential of 29.8 for CH_4 [11]. Figure 8 shows the CO_2eq for both engines and all load modes. With the ME3 the CO_2eq is lower than with ME4. At higher engine load of 50-90%, CO_2eq is 7-9% lower with ME3 compared to ME4, while at lower engine loads the difference is even more, ME3 producing 18% lower CO_2eq at 10% load and 25% load, compared to ME4.

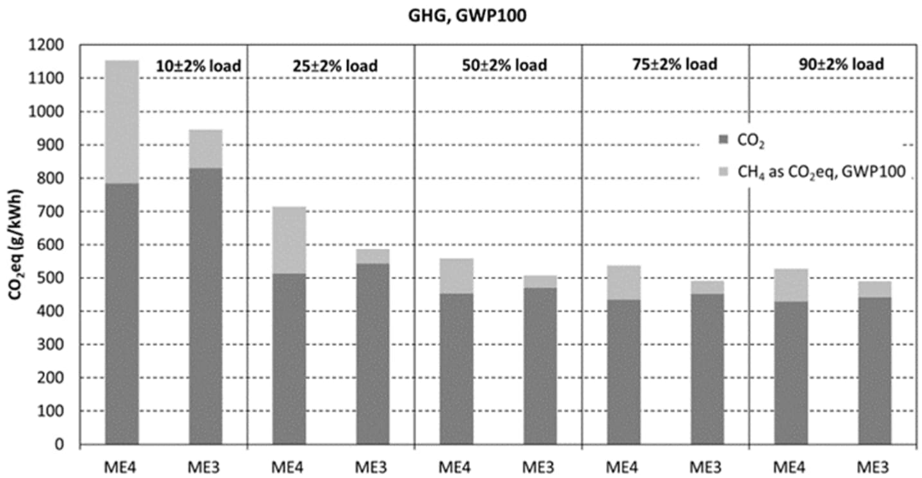

Figure 8 Total greenhouse gas emissions calculated based on measured CO_2 and CH_4 emissions as CO_2 equivalents for both engines ME4 and ME3 at different engine load conditions. 100-year global warming potential (GWP100) was used to convert methane emissions to CO_2 equivalents.

4.1.4. Methane slip under normal engine operation

Methane slip during normal engine operation was studied during one measurement day which included two whole journeys between Vaasa and Umeå shown in Figure 9.

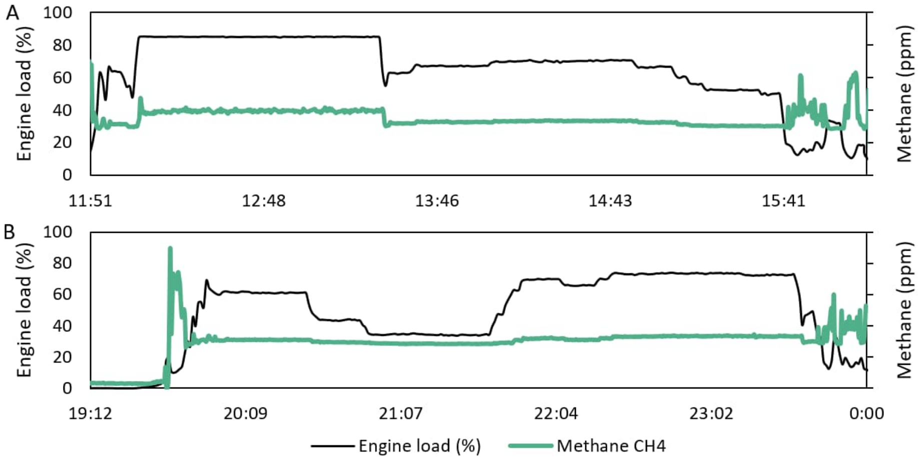

Figure 9. Behavior of methane concentrations measured on-board modern Ro-Pax ferry Aurora Botnia from engine piloting new combustion concept (ME3) during two voyages Umeå-Vaasa (A) and Vaasa-Umeå (B). The results from ME3 at different engine load conditions during stable engine operation are shown in Figure 5.

It could be seen that the frequent voyage of appr. 5h between the two harbors contained relatively more maneuvering operations at low loads and engine load was adjusted more frequently. The Ro-Pax ferry was also equipped with batteries and shore power use, enabling it to run down engines in harbors.

4.2. On board campaign #2 / Cruise Ship World Europa

In the second on-board campaign, methane, together with other gaseous and particulate emissions were studied under steady engine load conditions both during LNG and MGO operation. In addition, methane emissions under normal engine operation were studied during LNG operation.

4.2.1. Methane and other gaseous emissions under steady load conditions

4.2.1.1. LNG operation

The emissions of methane, ethane, propane, and ethene measured during steady engine load conditions are shown in Figure 10.

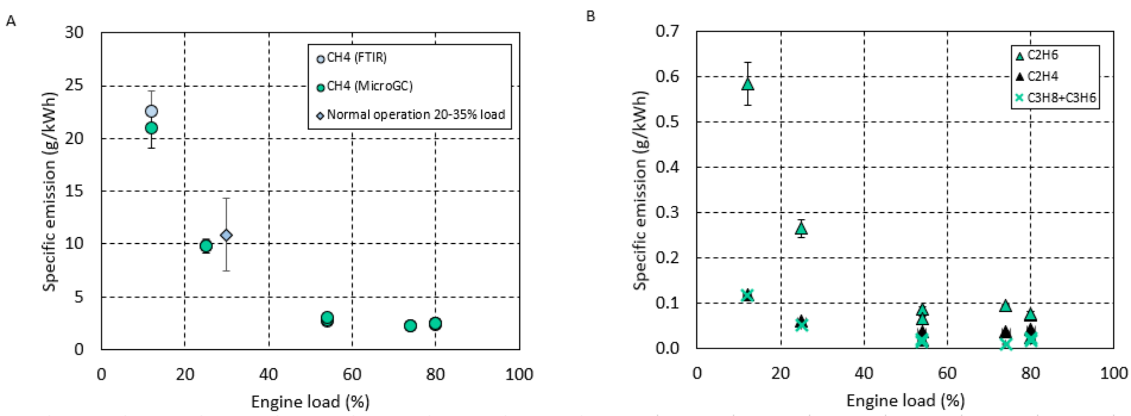

Figure 10. (A) Specific emissions of methane (CH_4) and (B) ethane (C2H6), propane (C3H8), and ethene (C2H4) measured under steady engine load conditions. Methane emission during normal engine operation under transient loads of 20-35% is shown for comparison (diamond marker). Standard deviation of the measurement is shown with error bars.

The methane slip measured under load conditions between 54-80% was between 2.3-3.0 g/kWh, whereas increased brake-specific emissions of 10 g/kWh and 21 g/kWh were observed at lower engine loads of 25% and 12%. Good agreement between the gas chromatography and FTIR methods were seen, however, during the low load condition of 12%, the methane concentrations were less stable and 1.5 g/kWh discrepancy between the methods was observed which was still within the standard deviation in this load condition. Methane emission measured during normal engine operation at 20-35% loads is shown for comparison (see Figure 13 and Figure 14 and related discussion). The 54% and 80% load condition measurements, which were repeated on separate days, were also in good agreement. The specific emissions of ethane, propane, and ethene were low in comparison to methane, in most cases below 0.1 g/kWh at all load conditions. However, at low load conditions of 25% and 12%, ethane emissions of 0.3 g/kWh and 0.6 g/kWh were observed, respectively. Out of the hydrocarbon concentrations measured from the exhaust, the share of methane varied between 94-97%, and shares of ethane, propane, and ethene between 2-4%, 0.5-1.6%, and 0.4-0.8% respectively. The shares reflect the composition of the LNG bunkered by the vessel, which had 97.6 mol-% methane, 1.9 mol-% ethane, and 0.24 mol-% propane.

During LNG operation, the specific emissions of carbon monoxide and formaldehyde (Table 7), were on constant levels at 54-80% load conditions, but exhibited similar load dependency as methane showing increased levels towards the low load conditions. Also increased CO_2 emissions were observed at low loads, while they remained constant (450-475 g/kWh) at 54-

80% load conditions. NO_x emissions varied according to engine load condition, and lowest levels were reached at highest engine load (1.2-1.3 g/kWh).

Table 7. Specific emissions of CO_2, CO, NOx, and HCHO during LNG and MGO operation. N_2O was measured but below detection limit (bd). During MGO operation, SCR was utilized as designed with urea injection on, while during LNG operation urea injection was not use.

	Load (%)	CO2 (g/kWh)	CH4 (g/kWh)	CO (g/kWh)	NO (g/kWh)	NO2 (g/kWh)	NOx (g/kWh)	HCHO (mg/kWh)		Load (%)	CH4 (g/kWh)	CO2 (g/kWh)	CO (g/kWh)	NO (g/kWh)	NO2 (g/kWh)	NOx (g/kWh)	HCHO (mg/kWh)
LNG	80	450	2.5	1.3	0.8	0.5	1.3	169	MGO	80	bd	602	0.3	12.9	0.6	13.7	bd
	80	449	2.5	1.3	0.8	0.4	1.2	170									
	75	451	2.3	1.2	1.5	0.5	2.1	162		75	bd	629	0.4	8.6	0.4	9.1	bd
	54	470	2.8	1.4	2.7	0.5	3.2	177		54	bd	642	0.4	9.8	0.5	10.4	bd
	54	475	3.0	1.4	2.8	0.5	3.3	182		54	bd	640	0.4	9.5	0.3	9.9	bd
	25	577	9.8	3.6	2.2	0.7	3.0	437		25	bd	745	0.8	11.5	0.8	12.4	bd
	12	861	21.1	8.7	3.3	1.1	4.4	959		10	0.024	1108	3.3	10.5	1.6	12.2	72
LNG (after SCR, no urea)	80	449	2.4	1.6	1.3	0.01	1.3	15	MGO (after SCR)	80	bd	601	0.4	6.6	0.03	6.8	bd
	80	449	2.4	1.5	1.3	0.01	1.3	12									
	75	451	2.2	1.4	2.1	0.01	2.1	14		75	bd	629	0.7	2.4	0.01	2.4	bd
	54	470	2.7	1.8	3.3	0.02	3.3	bd		54	bd	642	0.8	2.0	0.01	2.1	bd
	54	474	2.8	1.8	3.4	0.03	3.4	bd									
	25	575	10.1	5.2	3.4	0.03	3.5	bd		25	bd	744	1.7	2.0	0.02	2.0	bd
	12	856	20.3	12.1	4.3	0.04	4.4	bd									

4.2.1.2. MGO operation

The dual-fuel engines are also capable to operate on liquid fuel, and for comparison, the specific emissions (Table 7) were measured also during MGO-fueled engine operation. For methane, the concentrations measured during MGO operation were below detection for the micro gas chromatograph. With FTIR, the concentrations were also below the 2 ppm detection limit (corresponding to 0.007-0.008g/kWh) at 25-80% loads and 0.024 g/kWh was measured at 12% load. For CO, less pronounced load dependency was observed compared to LNG operation and overall levels were lower, specific CO emissions varying between 0.3-3.3 g/kWh for MGO and between 1.3-8.7 g/kWh for LNG over the measured load range. For formaldehyde, only the level at 12% load was above detectable amount, resulting in 72 mg/kWh compared to 170-960 mg/kWh detected during LNG operation. The benefits of LNG operation were visible in terms of NO_x emissions during MGO operation (upstream SCR), which ranged between 9-14 g/kWh. Also, in the liquid fuel mode with MGO, the CO_2 emissions were increased compared to LNG, being 602-640 g/kWh at 54-80% loads, and similarly to LNG, higher at lower engine loads.

During MGO operation, the methane slip values were low as expected and only the concentration at 10% load was above detection limit. In Fuel EU Maritime, 0.00005 gCH_4/gfuel is assumed for MGO at 50% load. Also formaldehyde was in most cases below detection and CO emissions also lower than during LNG operation. However, in terms of CO_2 and NO_x, the benefits of LNG operation were clear as LNG combustion decreased CO_2 emissions by 22-28% and engine-out NO_x by 64-90% depending on load condition. As expected, the use of SCR decreased the NO_x emissions during MGO operation and 2.0-2.4 g/kWh were measured at 25-75% loads. However, at the highest load condition of 80%, the NO_x remained at 6.8 g/kWh.

4.2.1.3. SCR effects

The studied engine was equipped with SCR system and FTIR was applied to study gaseous emission concentrations also downstream the SCR. The main purpose of the SCR, which is based on a catalytically induced reaction between NO_x and urea injected to the system, is to reduce NO_x to nitrogen during MGO operation. As during LNG operation, the NO_x emissions are naturally lower, the urea injection to the catalyst was only applied during MGO operation. Due to low exhaust temperature, the urea injection was not used either during the 10% operation condition with MGO. From Table 7, it can be seen that during

MGO operation, the SCR reduced total NO_x by 50-84% and decreased the fraction of NO_2. While during LNG operation, without the urea injection, no reduction in total NO_x was observed over SCR, some indications of catalyst activity were visible from the FTIR results, indicating conversion of NO_2 to NO with simultaneous increase in CO levels. Markedly, significantly lower formaldehyde levels were observed downstream the SCR, resulting in specific emissions of 12-15 mg/kWh or below the detection capability of the instrument, compared to 170-960 mg/kWh observed upstream the SCR system. Overall, with both fuels, methane and CO_2 emissions remained unaffected over the SCR system. With MGO, the methane concentrations were very low and partly below the detection level of the instrument.

4.2.2. Particle emissions under steady load conditions

4.2.2.1. LNG operation

In addition to gaseous emissions, particle mass, black carbon, and non-volatile particle number (Figure 11) were studied. For LNG operation, the particle emissions were generally on a low level, especially at the highest engine load conditions of 54-80%. At these load conditions, PM emissions were between 4-6.5 mg/kWh and black carbon 0.37-0.44 mg/kWh. The number of non-volatile particles above 23 nm in size also exhibited low levels of $0.7\text{-}1.0\times10^{12}$ 1/kWh, however, two to three-fold emissions of $2.1\text{-}3.3\times10^{12}$ 1/kWh were observed when 10 nm particle size was considered. At lower engine load conditions, the brake-specific PM emissions increased to 9.9 mg/kWh at 25% load and 56 mg/kWh at the lowest load condition of 10-14%. Comparing to higher load operation, BC emissions doubled to 0.94 mg/kWh at 25% load condition and again to 2.1 mg/kWh at 10-14%, while remaining on a considerably low level. For particle number, small increases were detected at 25% load, but more considerable change was noticed at 10-14% load where $PN_{nv,>23nm}$ increased by approximately one order of magnitude to 1.5×10^{13} 1/kWh. Also, two magnitude difference was observed for $PN_{nv,>10nm}$ (3.11×10^{14} 1/kWh) in comparison to the high load conditions of 54-80%.

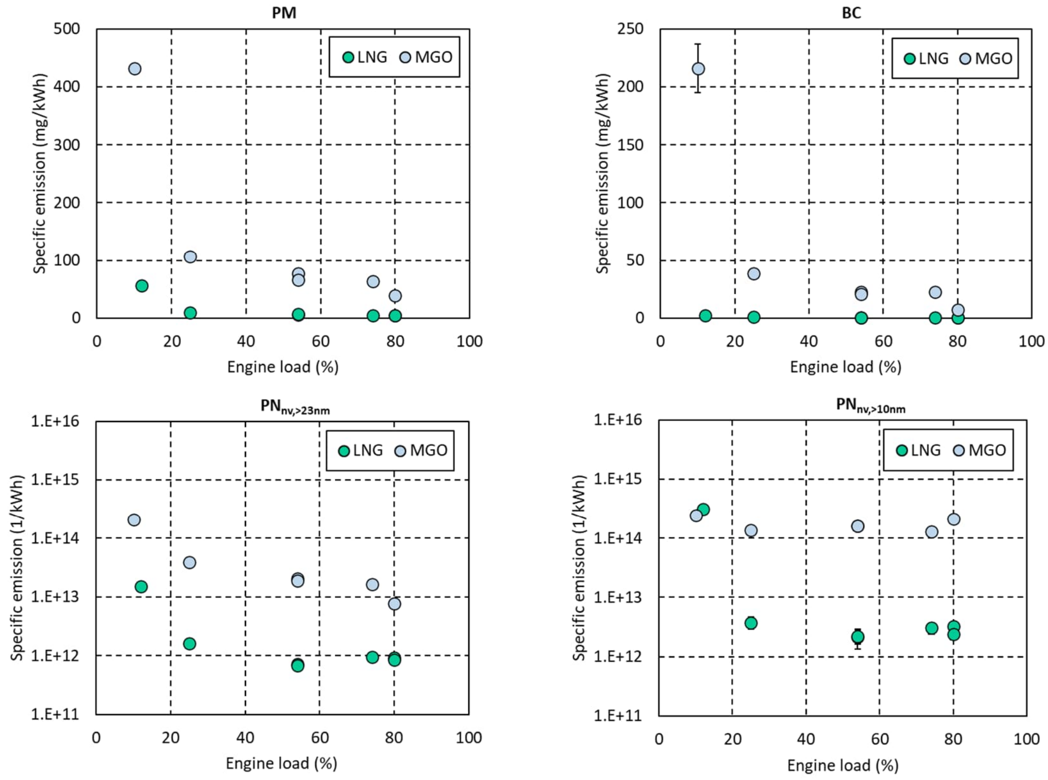

Figure 11. Specific emissions of black carbon (BC), particulate mass (PM), and number of non-volatile particles larger than 23nm ($PN_{nv,>23nm}$) or 10nm ($PN_{nv,>10nm}$) measured under steady load conditions while the engine was operated either in dual-fuel mode (LNG) or liquid fuel mode (MGO). Standard deviation of the measurement is shown with error bars. Note logarithmic axis in the bottom graphs.

4.2.2.2. MGO operation

During MGO operation (Figure 12), rather linear increase in PM and BC emissions were seen at 25-80% loads towards low load conditions, specific PM emissions varying between 39-107 mg/kWh and BC between 7.3-39 mg/kWh. At the lowest load condition of 10%, approximately 4-fold increase in PM and more than 5-fold increase in BC, compared to 25% engine load, was detected. The $PN_{nv,>23nm}$ varied between 7.7×10^{12} - 2.1×10^{14} 1/kWh over the studied loads increasing at low load conditions whereas $PN_{nv,>10nm}$ was more constant across the studied load range, varying between 1.3-2.5×10^{14} 1/kWh. These results indicate that increasing fraction of the PN resided between 10-23 nm size as higher engine loads were utilized.

4.2.3. Total greenhouse gas emissions including black carbon under steady load conditions

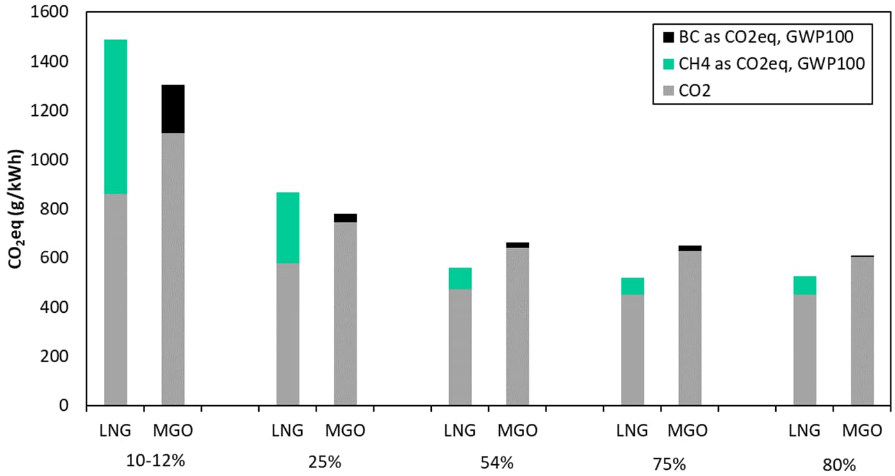

Figure 12. Specific emissions of greenhouse gases CO_2, CH_4 and black carbon, as CO_2 equivalents, considering the 100-year global warming potential for methane and black carbon under steady engine load conditions when the engine was operated in dual-fuel mode (LNG) or liquid fuel mode (MGO). Nitrous oxide (N_2O) was also measured but concentrations were below detection.

To consider the total greenhouse gas emission from the operation both on LNG and MGO, the specific CO_2 equivalent emissions were calculated considering methane and black carbon in addition to CO_2 (Figure 12). Overall, it was noticed that in the case of LNG operation, the contribution of black carbon to total CO_{2eq} GHG emissions was insignificant, and in the case of MGO operation, the corresponding observation was true for methane. At higher load conditions, 54% and above, methane contributed 13-15% of the total CO_{2eq} emission of the LNG combustion, but the contribution increased at low loads, being 34% at 25% load and 42% at 12% load condition. In the case of MGO operation, BC contributed 1-4% at loads between 25-80%, but also its contribution increased at low load to 15% of the total CO_{2eq}. Comparing the two fuels, it can be observed that at load conditions of 54% and above, 13-15% lower total CO_{2eq} (520-560 g/kWh) is achieved compared to MGO (610-660 g/kWh). However, at low loads, the increased methane slip results in 11-14% exceedance in total CO_{2eq} for LNG operation compared to MGO. N_2O was also measured but concentrations remained below the detection limit of the instrument (2 ppm). However, assuming the 2-ppm concentration for both fuels, corresponding to 0.00009-0.00015 g/g_{fuel}, would have resulted in approximately 1% increase in the total GHG emissions.

4.2.4. Methane slip under normal engine operation

In addition to steady engine load conditions, special attention during the campaign was given to the methane emissions occurring during normal engine operation. The load of the studied engine together with methane concentrations measured during these normal operation periods are shown in Figure 13 for the total period of the specific cruise.

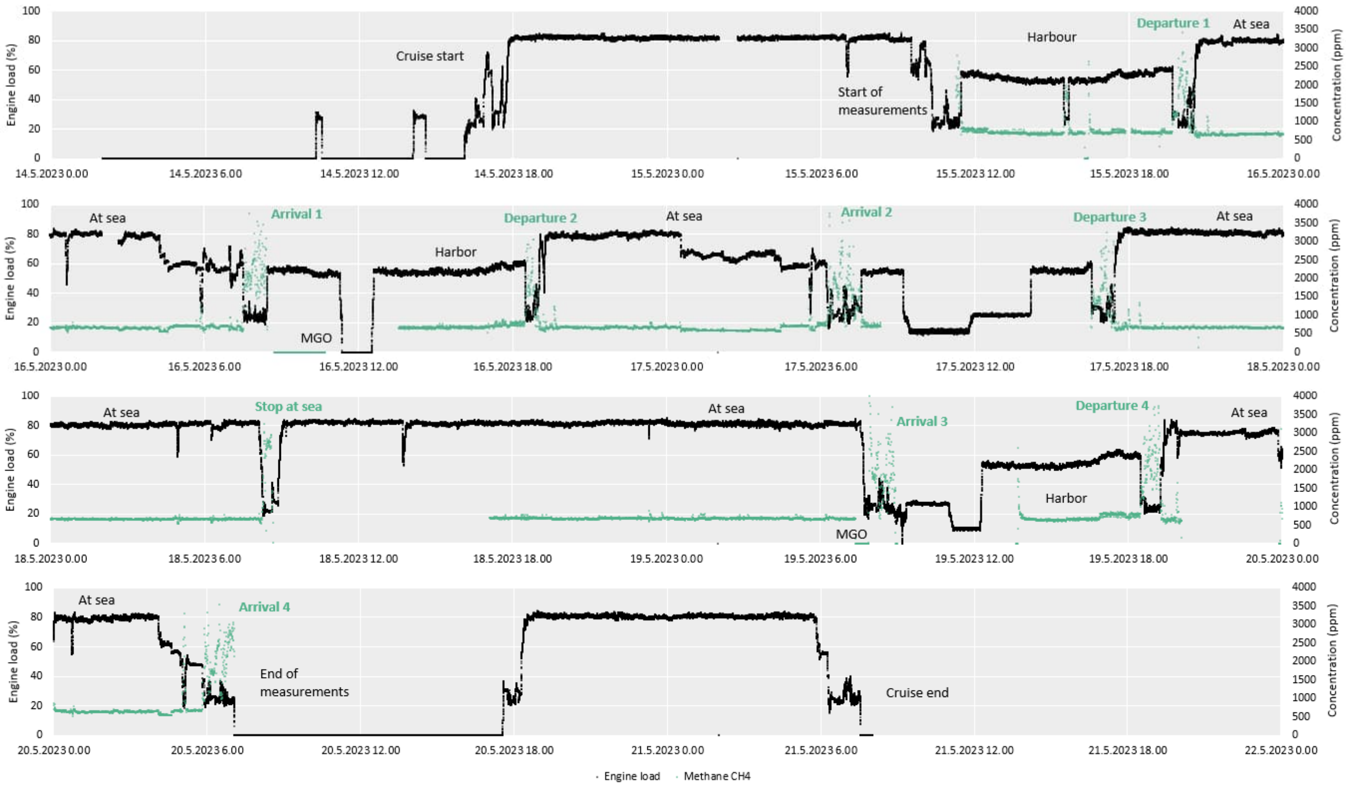

Figure 13. Engine load (in black, left axis) during the whole cruise and corresponding methane concentration (in green, right axis) for the periods when 'normal engine operation' was studied. During other periods of the cruise, either steady load condition was measured, or other activities took place (measurement instrument installations, calibrations etc.). Green annotations are used to mark the periods used for calculating an emission factor for the transient loads of 20-35% (shown in Figure 10).

In closer look, two example periods are shown in Figure 14. Figure 14A shows the measured methane concentrations during stay in the harbor, during departure and cruising at sea overnight as well as during arrival to harbor the following day. At harbor, the engine was mainly utilized at 50-60% loads although also shortly at 30% load, and for an equally short period, MGO was utilized instead of LNG. At sea, the engine mainly operated at 70-82% loads except close to arrival when the load condition was around 60% but was frequently adjusted for short periods when needed. During departure from harbor, engine loads of 20-44% were utilized, whereas upon arrival, the load, once lowered, varied between 19-33%. In general, varying engine loads in maneuvering during departures and arrivals are needed to adjust to the power need of the propulsion system in harbor environment where the ship may need to accurately operate in narrow environment with currents and possibly other vessels and docks in the vicinity of the ship. In multi-engine ships, typically many engines are kept running during these periods to have redundant power and ensure safe operation.

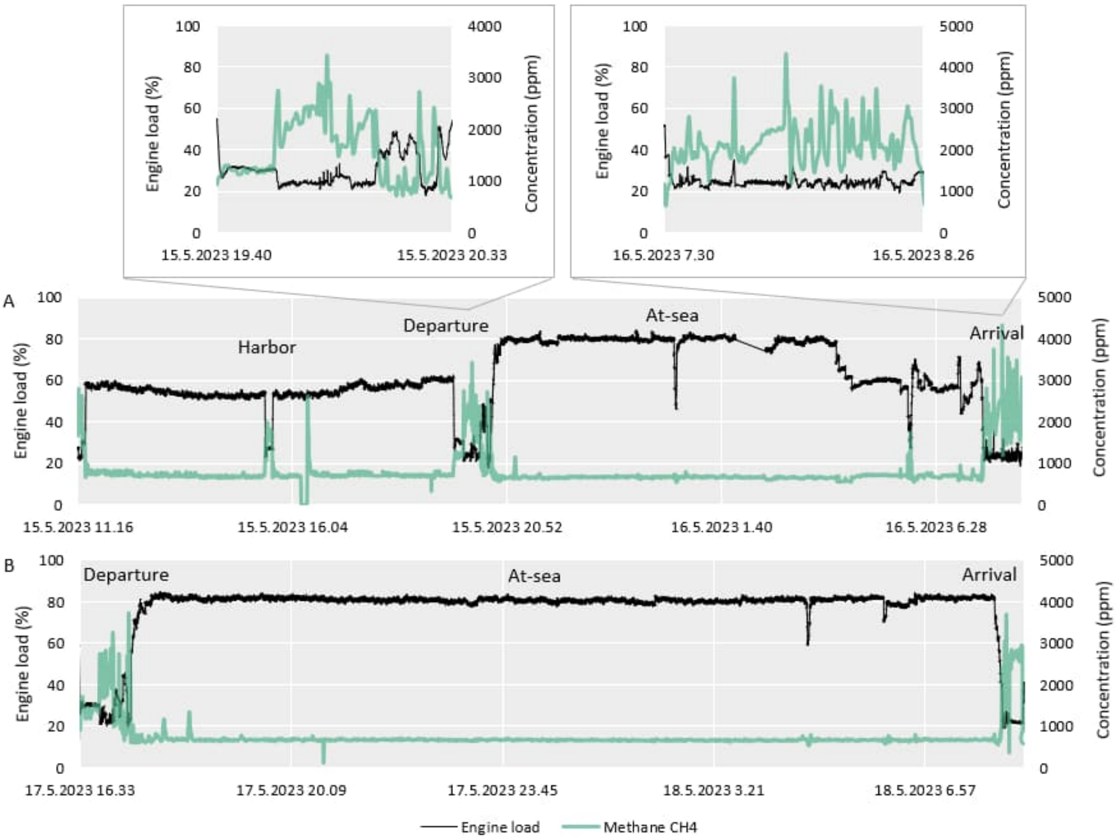

Figure 14. Example of engine load and methane concentrations measured during normal engine operation during docking in harbor, at sea, and during departures and arrivals. Engine load is logged in 1s intervals whereas methane concentration is measured as 20s averages.

Regarding methane concentrations in the exhaust, two observations can be made. Firstly, the immediate effect of the engine load is seen, as methane levels increased from the level of approximately 800 ppm to several fold when engine load was decreased to 20-35% level. Secondly, the fast changes in the engine load needed during arrivals and departures also caused corresponding fluctuation in the methane concentrations whereas during the steady engine load conditions the methane levels can be considered stable. During the short period when MGO was utilized by the engine, significantly lower methane concentration was observed as expected.

While increased methane concentrations could be observed during low load conditions, considering the normal vessel operation, the engine was operated on steady high load condition for prolonged periods (Figure 14B) when the vessel cruised at open sea. During these periods, the load remained considerably stable and methane levels in the exhaust remained on a stable level as well. Considering the total cruise, during normal vessel operation, only rare occurrences were seen where the engine was operated on a load condition below 20%.

To compare the increased and fluctuating methane levels observed during the transient engine operation during arrivals and departures, an emission factor for these periods, limited to time periods when the engine ran on 20-35% load was calculated and is shown in Figure 10 next to the emission factor measured during steady engine operation at 25% load condition. The obtained average methane emission of 10.9 g/kWh is about 11% higher than during steady 25% load. Due to the variable loads, higher standard deviation of 3.4 g/kWh was observed.

4.2.5. Methane slip under typical engine use during 8 months of vessel operation

As the brake-specific methane slip was found to increase at low engine loads but considering the engine use during the full cruise, it was visible that low load conditions were seldomly used, a weighted emission factor for methane was developed, applying the engine load condition data retrieved from the specific engine on the ship during 8 first months of the vessel operation. Figure 15A shows the load profile of the engine together with the share of the emitted methane at each corresponding load condition during the first 8 months, when the vessel was sailing in the Mediterranean. For this analysis, the time spent at each load condition (reported for every 5th %-unit) was divided in five load range categories and emission results at the corresponding steady load conditions (Figure 1) utilized to calculate the weighted specific emission for methane (shown in Table 3). For comparison, specific weighted emissions were calculated also according to the adjusted E2 cycle (Figure 15B) and adjusted D2 cycle (Figure 15C).

From the 8-month actual operation data for this vessel (Figure 15A), it can be seen that the engine is most typically operated on high load conditions of 80-85%, which contributes 39% of the total operation time. The load ranges of 65-75%, 40-60%, and 20-35% then contributed 21%, 31%, and 8% of the total operation time, respectively. The engine utilization at the lowest load conditions of 10-15% contributed less than 1% of the operation time. The operation profile was also reflected in the share of emitted methane as 43% of the total methane slip during the 8-month operation resulted from the engine operation at the highest load range, followed by contributions of 19%, 27%, and 10% from the operation at 65-75%, 40-60%, and 20-35% loads. For this vessel, the operation at 10-15% then contributed only 1% of the methane slip. Comparing with the E2 and D2 cycles (Figure 15 B, C), for main and auxiliary engines, it can be noticed that for this engine, the actual operation includes higher share of the high load conditions, and the mid-loads and highest loads are emphasized instead of the 75% load for which highest weight is given in the E2 cycle. The contribution of lowest load condition and corresponding methane slip is also significantly lower than in D2 cycle, however, it must be noted that while the same engine model is certified both for E2, and D2 cycles, in this specific ship it was applied as main engine, whereas the D2 cycle targets to reflect the engine use as an auxiliary engine.

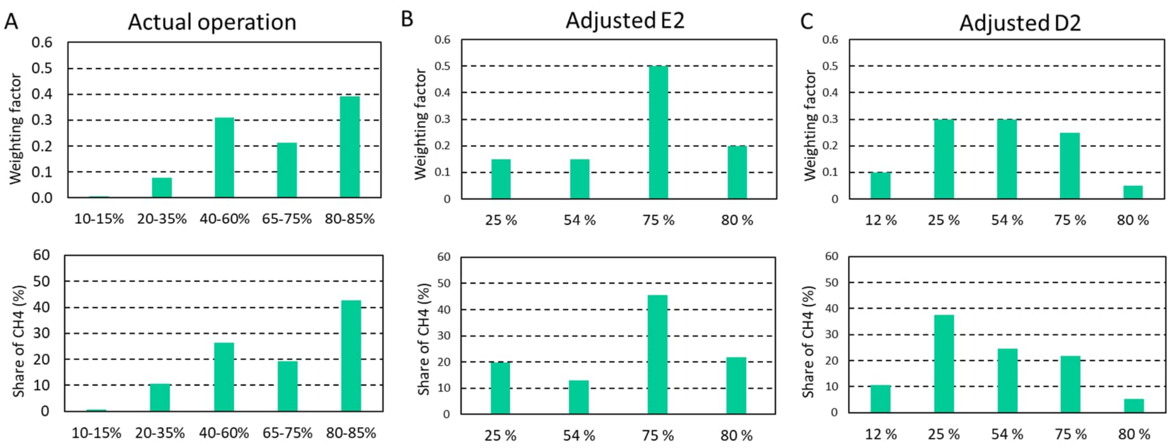

Figure 15. Real-world load profile of the engine during 8 months of vessel operation at the Mediterranean and distribution of methane slip produced at different load conditions (A), together with corresponding values for adjusted E2 (B) and D2 (C) test cycles. Weighting factor represents the share of operation time at certain load condition.

Despite the differences in the weighting factors seen in Figure 15, when considering the weighted emissions in brake-specific terms (g/kWh) and as percentage of consumed fuel (Table 8) the results align when comparing the real-world operation, E2 cycle, and the emission at 50% engine load, which is the definition applied in the FuelEU Maritime regulation. However, comparing to the D2 cycle, it could be noted that if operated as assumed in auxiliary engine use, the weighted methane slip as percentage of fuel use would be 41% higher than the real-world operation of the engine in the studied ship. Corresponding observations can be made regarding the total GHG emissions including CO_2 and BC, where the weighting according to 8-month real-world operation and E2 cycle give 544 gCO_{2eq}/kWh, 50% engine load 559 gCO_{2eq}/kWh, and the D2 cycle 609 gCO_{2eq}/kWh, 13% more than the real-world operation.

Table 8. Comparing weighted specific emission factors of methane and total GHGs including CO_2, methane, and BC under the real-world operation, according to adjusted E2 and D2 test cycles as well as at 50% engine load.

	Real-world operation	Adjusted E2 cycle	Adjusted D2 cycle	50% load
Methane (g/kWh)	2.8	2.8	4.3	2.9
Methane (% of fuel)	1.7	1.7	2.4	1.7
GHG (gCO_2eq/kWh)	544	544	609	559

In the case of the specific cruise vessel studied here, the low load operation had a small contribution to total engine operation time during 8 months of vessel operation, and the LNG use can be considered to bring a climate benefit even when accounting the methane slip. Also, while the analysis presented in Figure 15 considers methane, similar observations can be made regarding other emission compounds. As due to the high operation time, the load conditions of 40-85% contributed to 89% of the methane slip and special focus should be given to cutting methane slip at these load conditions where small improvements in brake-specific methane slip can have significant effect on the total emission. This result may reflect the typical engine operation on a cruise ship or more widely in ships with diesel-electric propulsion where engine load can be regulated by adjusting to the power need by alternating the number of engines in operation. However, the in-use engine load profile may not reflect vessels with different operation purposes. For example, as discussed by Peng et al. (2020), ferries may spend prolonged time at low load or idle while in port. In addition, engine use is likely to differ for ships which have direct propulsion systems. In vessels, where engines are frequently operated on low load conditions, special attention should be given to mitigation of the methane slip on low loads. In previous studies, shore power and batteries were suggested as complimentary strategies to reduce the utilization of low engine loads (Peng et al., 2020; Rochussen et al., 2023). Also modified injection timing, engine recalibration and novel combustion concept have been demonstrated on-board for reducing methane slip across low loads (Peng et al., 2020) and all engine load conditions (Rochussen et al., 2023).

Overall, in this study, the weighted methane emission for the actual operation of the ship was consistent with the results from the adjusted E2 cycle and the 50% engine load value which is applied in the FuelEU Maritime regulation whereas the D2 cycle representing auxiliary engine use resulted in 41% higher specific emission. Previously, Peng et al. (2020) used similar approach to compare weighted emission according to actual operation data collected during two weeks of vessel operation which showed that actual operation resulted in 74% higher emission than the E2 cycle. However, in a follow-up study (Rochussen et al., 2023) where new operation strategies were demonstrated, the E2 overestimated the CH_4 emission by 8% and by 30% after new engine calibration. In the study by Peng et al., (2020) the coastal vessel spent more than half of its operation time at loads above 50%, but also significant share of the operation time (32%) at idle, significantly different compared to the vessel in this study. It should be noted that, as seen in Figure 5, the actual load profile of the cruise ship studied here includes different load ranges whose shares vary from the E2 cycle as well as the assumption of the 50% engine load. Thus, direct causality of the consistency between the actual operation weighted emission with the E2 cycle and 50% load condition cannot be demonstrated here and more research would be needed to show whether the 50% load condition applied in the FuelEU maritime regulation reflects more generally the actual operation of other vessels with different engine configurations and activities.

The FuelEU Maritime regulation applies a default methane emission of 3.1% of fuel use for LPDF 4-S engines and also considers methane from emissions from MGO combustion. In IMO draft Guidelines for GHG Intensity of Marine fuels, 3.5% is used. Recently, increasing the default emission has been suggested based on comprehensive drone measurements of 17 vessels utilizing LPDF 4-S engines where methane slip varied between 1-14% with a median of 6.05% of fuel consumed (Comer et al., 2024). In this study, the methane slip weighted according to the actual operation profile of the engine (1.7% of fuel consumed) is 45% lower than the default value in FuelEU Maritime (3.1%) and markedly lower than a recently proposed value of 6% (Comer et al., 2024). Different measurement methodologies were used in these studies, however, Comer et al., (2024) showed rather good correlation between stack and drone measurements and more significant reason for the different findings is likely to be the different operation conditions considered. Also in this study, the break specific methane emission at varying 20-35% loads during normal vessel operation was found to be around 4 times higher than at 75-80% loads. While drone and stack measurements can complement each other, as drone measurements are conducted during momentary vessel operation and do not consider the whole operation profile of a specific vessel, they reflect the methane slip during certain operation conditions. E.g. Comer et al. (2024) reported the highest main engine load during their measurements to be 65% whereas the engine in this study operated 60% of time on load conditions above 65%. However, as discussed above, the results here reflect a cruise ship with diesel-electric propulsion and engine operation profiles may vary depending on vessel type. Considering the engine specific methane slip emissions at different engine loads, together with the real-life operation profile of the engine in the specific vessel could provide one methodology for defining the methane slip for different vessels. Considering the load specific emissions can also enable more accurate modelling of methane slip on a fleet level.

4.3. Comparison to other studies

Methane slip from LNG engines applying different engine technologies have been reviewed in D1.1. of the project (Kuittinen et al. 2023a). Here, methane slip and other emissions characterized during the on-board campaigns 1 and 2 could be compared to previous studies reporting results from on-board measurements focusing on the same engine type, LPDF 4-S engines. In Figure 16, methane slip is shown for the available studies, where engines manufactured in different years were investigated. The engine year is defined as the manufacturing year of the engine if mentioned in the specific study, or in most cases, as the building year of the vessel. Data for the newest engines from year 2021 as well as engine recalibrated in 2022 are shown separately in Figure 17.

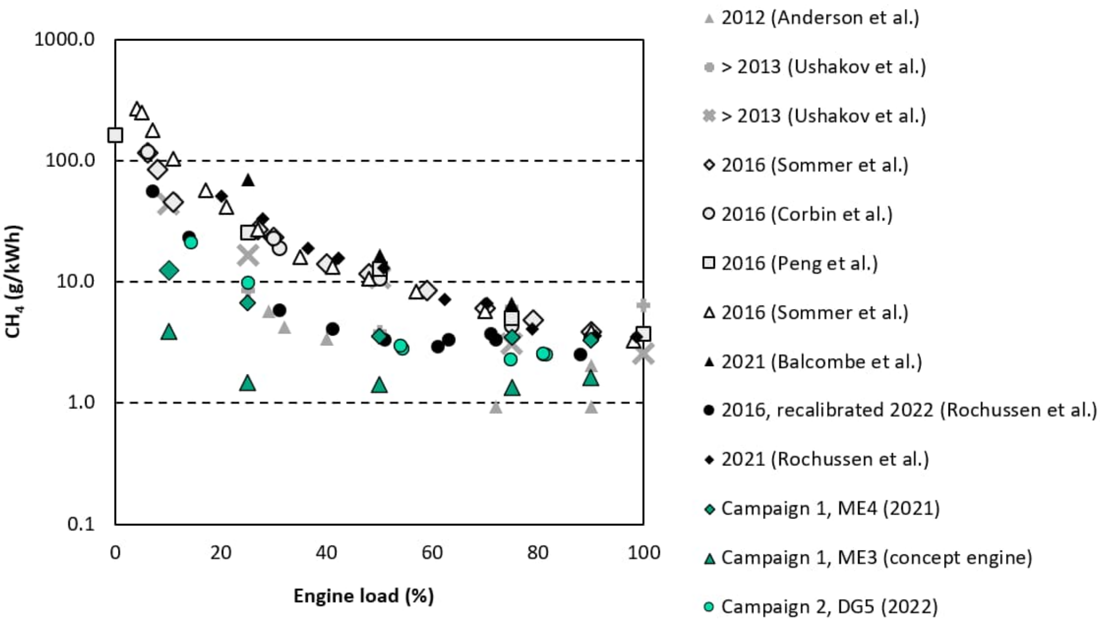

Figure 16. Methane slip measured under steady engine load conditions together with references showing methane slip reported from previous on-board studies for LPDF 4-S engines. Year of the studied engines is shown in the figure legend. Note the logarithmic vertical axis.

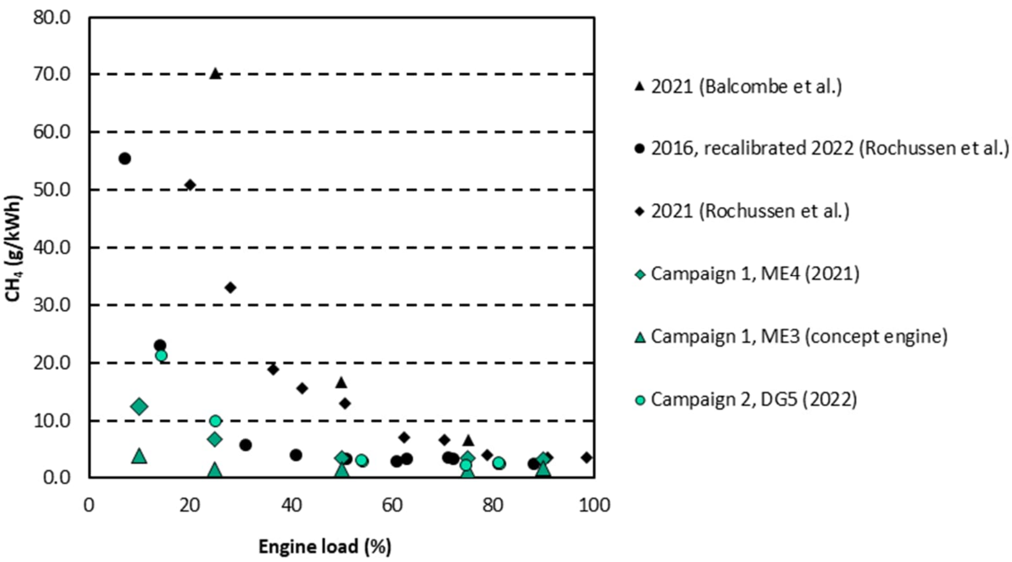

Figure 17. Methane slip measured under steady engine load conditions together with references showing methane slip reported from previous on-board studies for LPDF 4-S engines. Year of the studied engines is shown in the figure legend as well as engine configuration and bore size if given in the respective study.

Considering the methane slip across the studied engines loads between 12-80%, a load dependency in the specific methane emissions was observed, similarly to previous studies which have studied methane emissions from LPDF 4-S engines on-board (Figure 17). In earlier studies the methane slip has been reported from engines built in 2012 until 2021 (Anderson et al., 2015;

Balcombe et al., 2022; Corbin et al., 2020; Peng et al., 2020; Rochussen et al., 2023; Sommer et al., 2019; Ushakov et al., 2019). The results from the standard engines ME4 and DG5 are within the results reported for a 2012 engine, new at the time of measurements (Anderson et al., 2015) and an engine from 2016 which has been later recalibrated (Rochussen et al., 2023). At low load of 10%, the lowest emissions from these engines were reached with the ME4. Considering also the ME3 engine piloting a new combustion concept, it could be seen that significantly lower methane slip was reached with the new concept, in comparison to the previous literature, as well as the new standard engines ME4 and DG5. Overall, the results from Campaign 1 and 2 are within the lower range of all values reported in the literature which also include new engines from 2021 (Balcombe et al., 2022; Rochussen et al., 2023). However, some low values of below 1 g/kWh have been reported by Anderson et al. (2015) at highest 72-90% load conditions. While the brake-specific methane slip was found to depend on the engine load conditions and elevate at 25% load and increasingly at 10-12% load, it could be noticed that the phenomenon is suppressed compared to previous on-board studies where up to 70 g/kWh and 103 g/kWh have been reported at 25% and 12% load conditions, respectively.

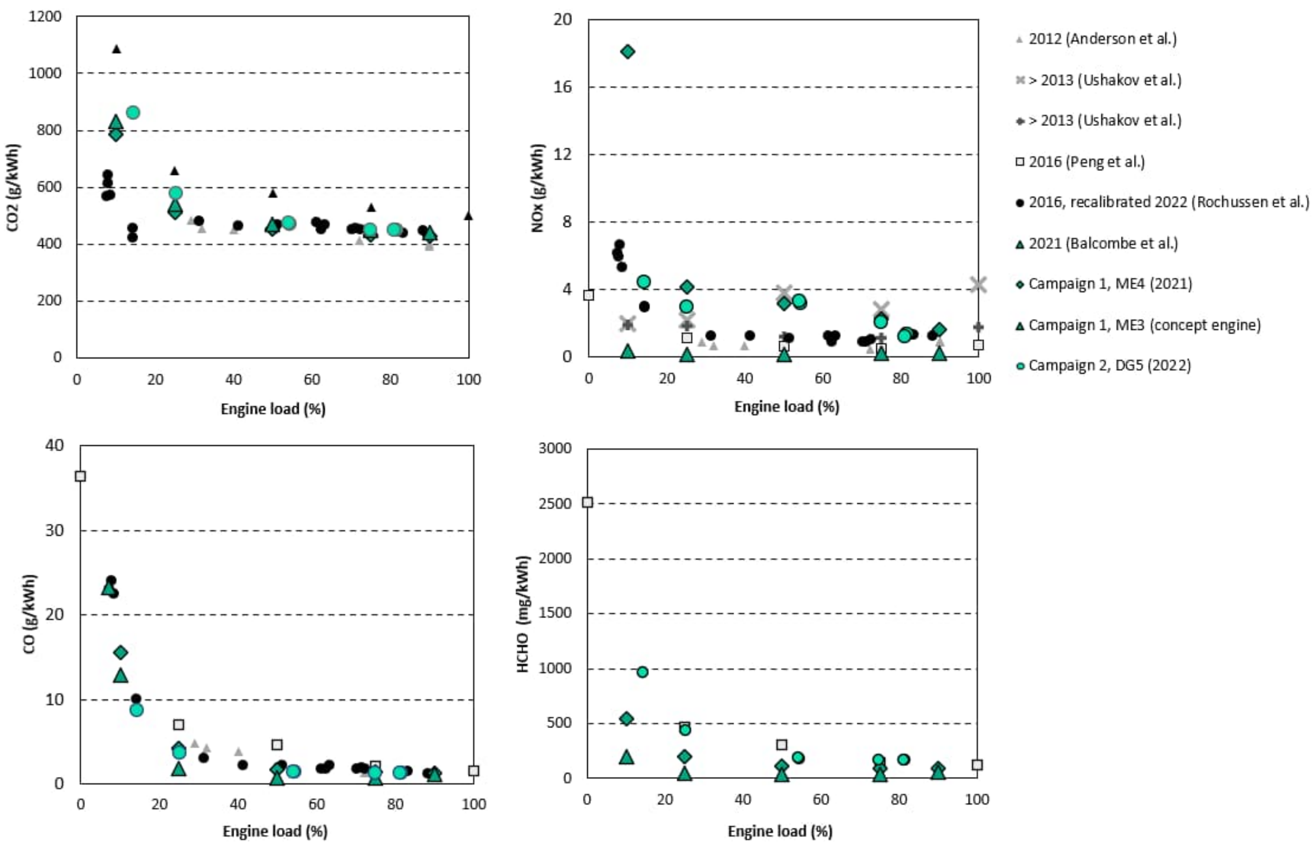

Figure 18. Carbon dioxide, nitrogen oxides, carbon monoxide, and formaldehyde measured under steady engine load conditions together with references showing gaseous emissions reported from previous on-board studies for LPDF 4-S engines. Year of the studied engines is shown in the figure legend.

The other gaseous compounds (Figure 18) measured during the on-board campaigns during LNG operation were within the previously reported values for LPDF 4-S engines. For CO_2, the values at 50-80% loads follow the values reported by Rochussen et al. (2023) for a newly calibrated engine, and Anderson et al. (2012), while Balcombe et al. (2022) reported somewhat higher levels over the whole load range. At lower load conditions, it can be seen that low CO_2 levels compared to those measured here have been achieved with the engine recalibration conducted in the study by Rochussen et al. (2023).

The NO_x emissions for the standard engines ME4 and DG5 varied between 1.3-4.1 g/kWh, being in the range reported before by Ushakov et al. 2019, however, being somewhat higher the values reported by Anderson et al. 2012, Peng et al. 2020 and Rochussen et al. 2023, where new engine calibration was applied. At the lowest load of 10-12%, the ME4 produced a higher specific emission of 18 g/kWh whereas the NO_x level for DG5 remained below the values reported by Rochussen et al. 2023 at 8% load. The results for the ME3 with new combustion concept showed that significantly low NO_x emissions below other literature values were reached, 0.2-0.3 g/kWh at 25-90% loads and 0.4 g/kWh at 10% load.

Regarding CO, the values measured from the standard engines ME4 and DG5 are well aligned with previous studies by Anderson et al. (2012) and Rochussen et al. (2023) at load conditions above 25% whereas Peng et al. (2020) reported somewhat higher values. Lowest CO emissions at these loads were reached with ME3 new combustion concept engine. At lowest loads of 10-12%, the CO levels measured in this study remained below the previously reported values.

Formaldehyde from LPDF 4-S engines has previously been measured on-board in only one study. Peng et al. (2020) showed 120-440 mg/kWh with levels increasing as load decreased from 100% to 25%, and at idle, 2500 mg/kWh was reached. In Campaign 1 for ME3 and ME4, formaldehyde was calculated as hydrocarbons, according to the NOx technical code, and 50-550 mg/kWh were found for standard engine and 50-200 mg/kWh for an engine piloting a new combustion concept. In Campaign 2 for DG5, molar mass-based density was applied to formaldehyde, explaining the approximately two-fold levels. Considering this, the findings here align with the previous study of Peng et al. (2020) at the load conditions considered. Complying with tighter emission limits for NO_x is currently required for new ships in the Nitrogen Emission Control Areas (NECAs) which comprise the North American and Caribbean NECAs as well as the North Sea and Baltic Sea NECAs (IMO, 2022). In Campaign 2, SCR system was installed in the exhaust channel to reduce NO_x levels during MGO operation of the dual-fuel engine, however, indication of the system affecting the exhaust composition during LNG operation could be noticed even without the urea injection. Specifically, the emissions of formaldehyde and NO_2 decreased downstream the SCR system. Formaldehyde is a carcinogen which is linked to health effects such as asthma and nasopharyngeal cancer, as well as photochemical smog and ground-level ozone formation in the atmosphere with their related health effects (Peng et al., 2020 and references within). In their study, (Peng et al., 2020) conducted a health risk assessment of LNG exhaust compared to MGO and while they found that maximum individual cancer risk and chronic non-carcinogenic health index were reduced by 92% and 35% at LNG operation, and an 8-hr chronic hazard index increased more than 6-fold with LNG due to increased formaldehyde levels. When they assumed 95% removal of formaldehyde by the use of an oxidation catalyst, the health indexes were 63-94% lower for LNG than for diesel operation.

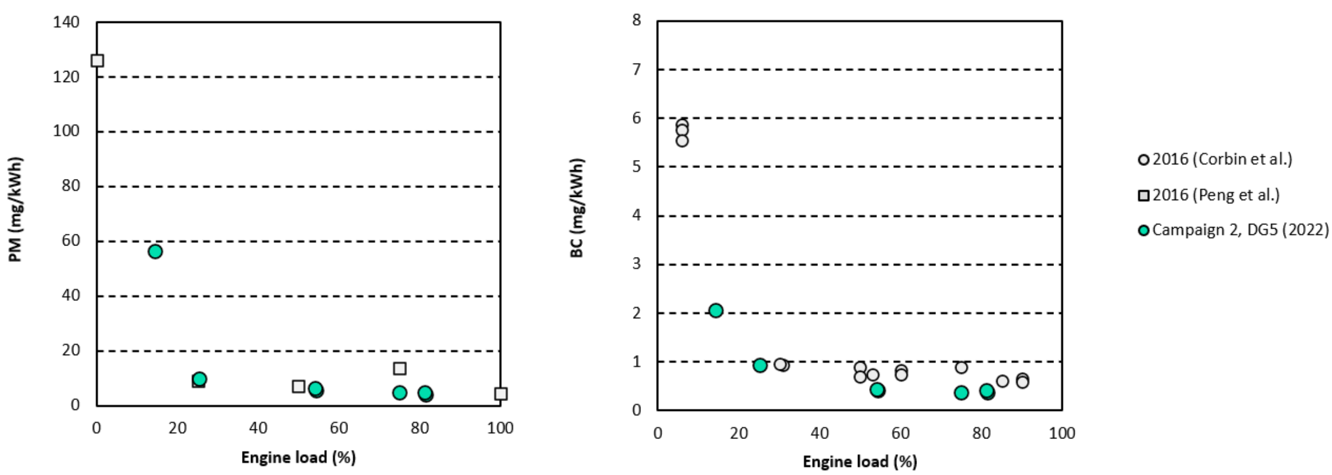

Figure 19. Particle mass and black carbon measured on-board Campaign 2, together with references showing results reported from previous on-board studies for LPDF 4-S engines. Year of the studied engines is shown in the figure legend.

Particle mass and black carbon (Figure 19) were measured from DG5 in Campaign 2. The particle mass results from LNG combustion at 25-54% and 80% loads for DG5 are similar to the observations of Peng et al., (2020) who collected PM samples of 7-9 mg/kWh at 25-50% loads and 4.5 mg/kWh at 100% load. However, lower PM emission is observed here at 75% load, 5mg/kWh compared to 14 mg/kWh. From laboratory studies, higher values of 20 mg/kWh and 32 mg/kWh have earlier been reported for a retrofit engine at 85% and 40% loads respectively, and 10 mg/kWh at 75% load for a production engine (Lehtoranta et al., 2019). In our study, increased level of 56 mg/kWh was observed at 10-14% load condition, whereas it remained lower than the observation of 126 mg/kWh reported by Peng et al. during engine idle. Corbin et al. reported black carbon emissions from the same campaign as (Peng et al., 2020). Here, the results for BC at 55-82% load (0.4 mg/kWh) are lower than reported earlier (0.6-0.9 mg/kWh) but on a similar level at 25% load. In this study, BC was observed to increase to 2 mg/kWh at 12% load whereas Corbin et al. (2020) reported up to 6 mg/kWh at 6% load condition.

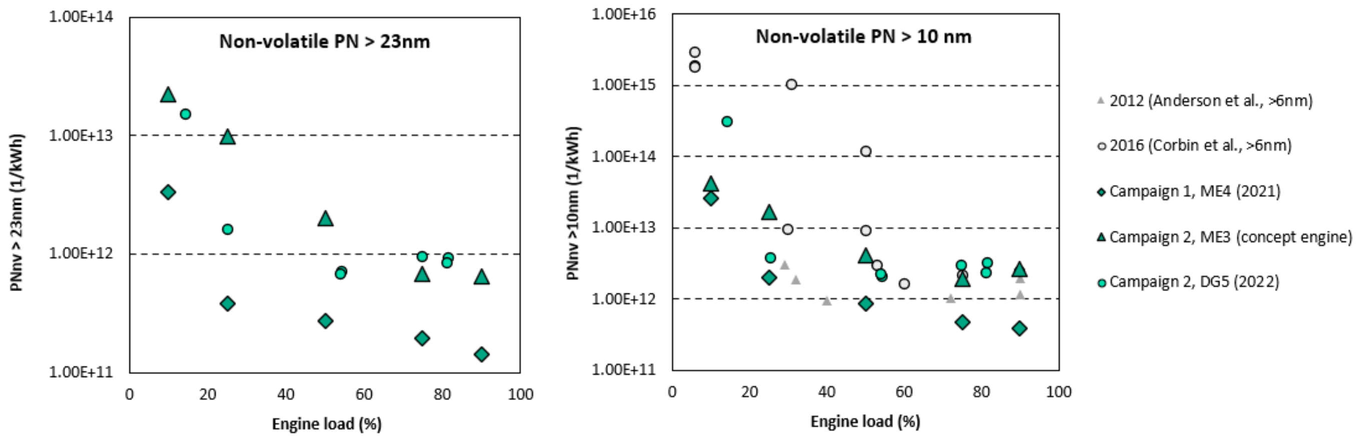

Figure 20. Non-volatile particle number above 23 nm and above 10 nm in size, together with references showing particle number results reported from previous on-board studies for LPDF 4-S engines. Note that the reference values for PNnv >10nm have consider lower cut-off value of 6 nm in their studies. Year of the studied engines is shown in the figure legend. Not logarithmic vertical axis in the figures.

In previous literature considering on-board measurements of methane slip from LPDF 4-S engines, no simultaneous recordings of non-volatile particle number above 23 nm or 10 nm were found. However, Anderson et al. (2012) and Corbin et al. (2020) have reported non-volatile PN for particles sized above 6 nm which was compared with the $PN_{nv,>10nm}$ studied here. (Figure 20) For all the studied engines, the $PN_{nv,>23nm}$ was below 1×10^{12} kWh^{-1}, a limit value set for inland ships, at engine load conditions of 75-90% and at 50% for the standard engines ME4 and DG5. At the lowest loads however, an increase of one magnitude to above 10^{13} kWh^{-1} was visible. Considering particle number until the particle size of 10 nm at 50-90% loads, it could be seen that $PN_{nv,>10nm}$ levels were between 10^{12} -10^{13} kWh^{-1} for ME3 and DG5, whereas for ME4 also they remained below the 1×10^{12} kWh^{-1} limit value. At low load conditions, the $PN_{nv,>10nm}$ levels were increased above 10^{13} kWh^{-1} and above 10^{14} kWh^{-1} in case of DG5 but remained lower that the earlier values reported by Corbin et al. (2020). In earlier laboratory studies, natural gas combustion has been shown to produce particles with diameters in the ultrafine and nano particle size (e.g. Alanen et al., 2020). Also in this study, where count of particles larger than 23nm and 10nm could be compared, significant fraction of the total $PN_{nv,>10nm}$ were smaller than 23 nm and thus remain uncounted when the 23nm cut-point is applied.

5. Conclusions

In this study, methane slip was determined from three LNG-fueled LPDF 4-S engines on-board two newly build vessels - a ferry constructed in 2021 and a cruise ship constructed in 2022. Overall, it was shown that the methane slip produced by the newbuild engines was in the lower range of values reported in the previous literature. Load dependency of the methane slip, as well as other emission compounds, were observed. At 50-90% engine loads, the new standard engines showed methane levels of 2.3-3.6 g/kWh and 6.7-9.8 g/kWh were recorded at 25% load and 12-21 g/kWh at 10-12% engine loads. The third engine piloting a new combustion concept could reduce methane slip to 1.4-1.6 g/kWh at 50-90% load conditions, 50-65% less compared to the standard engine of same size installed on the same vessel. At low load conditions, where the new combustion concept engine showed 1.5 g/kWh at 25% load and 3.9 g/kWh at 10% load, the difference was even higher.

Due to the load dependency of the methane slip, the contribution of methane to total CO_2 equivalent emissions increased at low loads. The results from the measurements conducted on a ferry showed that considering both CO_2 and methane, the new combustion concept engine brought benefits over the whole engine load range. In the measurements conducted on the cruise ship, also black carbon was considered, and comparison could be made with the engine combusting either LNG or MGO. LNG usage brought benefits in terms of total CO_2 equivalent emissions at load conditions of 54% and above but at lower loads, the benefits in terms of CO_2 and BC were undermined by the uncombusted methane.

Considering other emissions, the emissions of nitrogen oxides, carbon monoxide and formaldehyde were in line with previous literature values of on-board measurements of LPDF 4-S engines combusting LNG. For the new combustion concept engine, low emissions of nitrogen oxides were recorded compared to the standard engine, however with a simultaneous increase in particle number. At high loads above 75%, the number of non-volatile particles for all of the studied engines were under the limit value of 10^{12} kWh^{-1} defined for inland waterway vessels. Decrease in formaldehyde emissions over the SCR catalyst even without urea injection were recorded, suggesting that in vessels where SCR is installed downstream the dual-fuel engines, the SCR could provide an additional mitigation pathway for formaldehyde.

In both campaigns, in addition to steady engine load conditions, also the normal engine operation of the vessel was studied. The normal operation measured on-board suggests that in these ships, engines are rarely operated at very low loads. However, methane concentrations observed during normal engine operation indicated increased concentrations in the exhaust during arrivals and departures where lower engine loads are utilized and load frequently adjusted.

To consider the normal engine operation, the activity profile of the engine on-board the cruise ship could be observed during 8-months of vessel operation on the Mediterranean, and a weighted emission factor for methane was developed, resulting in 2.8 g/kWh for this specific ship. The weighted emission according to normal vessel operation corresponds to 1.7% of the fuel use, which is lower compared to the default value of 3.1% applied in the FuelEU Maritime regulation. This weighted emission factor represents the activity of the specific cruise vessel where the engine was operated at loads above 40% for more than 90% of the operation time. In this study, the actual operation weighted emission factor was consistent with the value at 50% load, used by the FuelEU Maritime, but this is seen to be rather a coincidence and studies lack showing more repeatability of the observation on larger number of vessels. For other vessel types with varying activity profiles, similar approach, combining load dependent emission factors at several load conditions and activity profile of the specific engine, could be applied. Together with engine development focusing on reduction of methane slip on the mostly utilized engine loads, operation strategies and load optimization could help to reduce methane emissions from LNG engines.

References

Alanen, J., Isotalo, M., Kuittinen, N., Simonen, P., Martikainen, S., Kuuluvainen, H., Honkanen, M., Lehtoranta, K., Nyyssönen, S., Vesala, H., Timonen, H., Aurela, M., Keskinen, J., & Rönkkö, T. (2020). Physical Characteristics of Particle Emissions from a Medium Speed Ship Engine Fueled with Natural Gas and Low-Sulfur Liquid Fuels. Environmental Science and Technology, 54(9), 5376–5384. https://doi.org/10.1021/acs.est.9b06460

Anderson, M., Salo, K., & Fridell, E. (2015). Particle- and Gaseous Emissions from an LNG Powered Ship. Environmental Science and Technology, 49(20), 12568–12575. https://doi.org/10.1021/acs.est.5b02678

Balcombe, P., Heggo, D. A., & Harrison, M. (2022). Total Methane and CO 2 Emissions from Liquefied Natural Gas Carrier Ships: The First Primary Measurements. Environmental Science & Technology, 56, 9632–9640. https://doi.org/10.1021/acs.est.2c01383

Bond, T. C., Doherty, S. J., Fahey, D. W., Forster, P. M., Berntsen, T., Deangelo, B. J., Flanner, M. G., Ghan, S., Kärcher, B., Koch, D., Kinne, S., Kondo, Y., Quinn, P. K., Sarofim, M. C., Schultz, M. G., Schulz, M., Venkataraman, C., Zhang, H., Zhang, S., … Zender, C. S. (2013). Bounding the role of black carbon in the climate system: A scientific assessment. Journal of Geophysical Research Atmospheres, 118(11), 5380–5552. https://doi.org/10.1002/jgrd.50171

Comer, B., Beecken, J., Vermeulen, R., Sturrup, E., Paschinger, P., Osipova, L., Gore, K., Delahaye, A., Verhagen, V., Knudsen, B., Knudsen, J., Verbeek, R., & 2024, J. (2024). FUGITIVE AND UNBURNED METHANE EMISSIONS FROM SHIPS (FUMES) Characterizing methane emissions from LNG-fueled ships using drones, helicopters, and onboard measurements. www.theicct.org

Corbin, J. C., Peng, W., Yang, J., Sommer, D. E., Trivanovic, U., Kirchen, P., Miller, J. W., Rogak, S., Cocker, D. R., Smallwood, G. J., Lobo, P., & Gagné, S. (2020). Characterization of particulate matter emitted by a marine engine operated with liquefied natural gas and diesel fuels. Atmospheric Environment, 220. https://doi.org/10.1016/j.atmosenv.2019.117030

European Commission. (2024). Reducing emissions from the shipping sector. https://climate.ec.europa.eu/eu-action/transport/reducing-emissions-shipping-sector_en

FuelEU Maritime. Regulation (EU) 2023 of the European Parliament and of the Council on the Use of Renewable and Low-Carbon Fuels in Maritime Transport, and Amending Directive 2009/16/EC. (2023).

Grönholm, T., Makela, T., Hatakka, J., Jalkanen, J. P., Kuula, J., Laurila, T., Laakso, L., & Kukkonen, J. (2021). Evaluation of Methane Emissions Originating from LNG Ships Based on the Measurements at a Remote Marine Station. Environmental Science and Technology, 55(20), 13677–13686. https://doi.org/10.1021/acs.est.1c03293

IPCC. (2022). Mitigation of Climate Change Climate Change 2022 Working Group III contribution to the Sixth Assessment Report of the Intergovernmental Panel on Climate Change. www.ipcc.ch

Kuittinen, N., Heikkilä, M., Jalkanen, J.-P., Aakko-Saksa, P., & Lehtoranta, K. (2023a). Methane slip emissions from LNG vessels-review. Proceedings of the 30th CIMAC World Congress 2023. https://www.cimac.com.

Kuittinen, N., Heikkilä, M., Lehtoranta, K. (2023b) Review of methane slip from LNG engines. Available at https://greenray-project.eu/wp-content/uploads/2023/04/D1.1_Review_of_methane_slip_from_LNG_engines.pdf

Kuittinen, N., Jalkanen, J. P., Alanen, J., Ntziachristos, L., Hannuniemi, H., Johansson, L., Karjalainen, P., Saukko, E., Isotalo, M., Aakko-Saksa, P., Lehtoranta, K., Keskinen, J., Simonen, P., Saarikoski, S., Asmi, E., Laurila, T., Hillamo, R., Mylläri, F., Lihavainen, H., … Rönkkö, T. (2021). Shipping Remains a Globally Significant Source of Anthropogenic PN Emissions even after 2020 Sulfur Regulation. Environmental Science and Technology, 55(1), 129–138. https://doi.org/10.1021/acs.est.0c03627

Lehtoranta, K., Aakko-Saksa, P., Murtonen, T., Vesala, H., Ntziachristos, L., Rönkkö, T., Karjalainen, P., Kuittinen, N., & Timonen, H. (2019). Particulate Mass and Nonvolatile Particle Number Emissions from Marine Engines Using Low-Sulfur Fuels, Natural Gas, or Scrubbers. Environmental Science and Technology, 53(6), 3315–3322. https://doi.org/10.1021/acs.est.8b05555

Lehtoranta, K., Kuittinen, N., Vesala, H., & Koponen, P. (2023). Methane emissions from a state-of-the-art LNG powered vessel. Atmosphere, 14(5), 825. https://doi.org/10.3390/atmos14050825

Peng, W., Yang, J., Corbin, J., Trivanovic, U., Lobo, P., Kirchen, P., Rogak, S., Gagné, S., Miller, J. W., & Cocker, D. (2020). Comprehensive analysis of the air quality impacts of switching a marine vessel from diesel fuel to natural gas. Environmental Pollution, 266. https://doi.org/10.1016/j.envpol.2020.115404

Rochussen, J., Jaeger, N. S. B., Penner, H., Khan, A., & Kirchen, P. (2023). Development and demonstration of strategies for GHG and methane slip reduction from dual-fuel natural gas coastal vessels. Fuel, 349. https://doi.org/10.1016/j.fuel.2023.128433

Sommer, D. E., Yeremi, M., Son, J., Corbin, J. C., Gagné, S., Lobo, P., Miller, J. W., & Kirchen, P. (2019). Characterization and Reduction of In-Use CH 4 Emissions from a Dual Fuel Marine Engine Using Wavelength Modulation Spectroscopy. Environmental Science and Technology, 53(5), 2892–2899. https://doi.org/10.1021/acs.est.8b04244

Stenersen, D., & Thonstad, O. (2017). SINTEF Ocean AS Maritim GHG and NOx emissions from gas fuelled engines. www.sintef.no/ocean

Ushakov, S., Stenersen, D., & Einang, P. M. (2019). Methane slip from gas fuelled ships: a comprehensive summary based on measurement data. In Journal of Marine Science and Technology (Japan) (Vol. 24, Issue 4, pp. 1308–1325). Springer. https://doi.org/10.1007/s00773-018-00622-z